Free Radical Biology and Medicine 188 (2022) 298–311

Contents lists available at ScienceDirect

Free Radical Biology and Medicine

journal homepage: www.elsevier.com/locate/freeradbiomed

The ROS-generating enzyme NADPH oxidase 1 modulates the colonic microbiota but offers minor protection against dextran sulfate sodium-induced low-grade colon inflammation in mice

Anne Mari Herfindal [a], Sérgio Domingos Cardoso Rocha [a,b], Dimitrios Papoutsis [a], Siv Kjølsrud Bøhn [a], Harald Carlsen [a,*]

[a] Faculty of Chemistry, Biotechnology and Food Science, Norwegian University of Life Sciences, P. O. Box 5003, N-1432, Ås, Norway
[b] Faculty of Biosciences, Norwegian University of Life Sciences, P. O. Box 5003, N-1432, Ås, Norway

ARTICLE INFO

Keywords:
Reactive oxygen species (ROS)
NADPH oxidase 1 (NOX1)
Dextran sulfate sodium
Gut inflammation
Intestinal microbiota

ABSTRACT

The enzyme NADPH oxidase 1 (NOX1) is a major producer of superoxide which together with other reactive oxygen and nitrogen species (ROS/RNS) are implicated in maintaining a healthy epithelial barrier in the gut. While previous studies have indicated NOX1's involvement in microbial modulation in the small intestine, less is known about the effects of NOX1-dependent ROS/RNS formation in the colon. We investigated the role of NOX1 in the colon of NOX1 knockout (KO) and wild type (WT) mice, under mild and subclinical low-grade colon inflammation induced by 1% dextran sulfate sodium (DSS). *Ex vivo* imaging of ROS/RNS in the colon revealed that absence of NOX1 strongly decreased ROS/RNS production, particularly during DSS treatment. Furthermore, while absence of NOX1 did not affect disease activity, some markers of inflammation (mRNA: *Tnfa*, *Il6*, *Ptgs2*; protein: lipocalin 2) in the colonic mucosa tended to be higher in NOX1 KO than in WT mice following DSS treatment. Lack of NOX1 also extensively modulated the bacterial community in the colon (16S rRNA gene sequencing), where NOX1 KO mice were characterized mainly by lower α-diversity (richness and evenness), higher abundance of Firmicutes, *Akkermansia*, and *Oscillibacter*, and lower abundance of Bacteroidetes and *Alistipes*. Together, our data suggest that NOX1 is pivotal for colonic ROS/RNS production in mice both during steady-state (i.e., no DSS treatment) and during 1% DSS-induced low-grade inflammation and for modulation of the colonic microbiota, with potential beneficial consequences for intestinal health.

1. Introduction

Reactive oxygen and nitrogen species (ROS/RNS) are reactive molecules produced by cells during normal cellular metabolism and their production can be triggered in cells of the innate immune system to kill bacteria [1–3]. They include superoxide ($O_2^{\bullet-}$), hydrogen peroxide (H_2O_2), hydroxyl radical ($^{\bullet}OH$), nitric oxide ($^{\bullet}NO$), peroxynitrite ($ONOO^-$), and hypochlorous acid (HOCl). Although ROS/RNS can lead to cellular damage and diseases their essential roles in cellular signaling are widely recognized [1–3]. Several enzymes are responsible for ROS/RNS production, with expression patterns and functions that vary depending on cell type [4].

During normal steady-state conditions in the intestine, NADPH oxidase (NOX) 1 (NOX1) and dual oxidase 2 (DUOX2) in epithelial cells are the primary sources of ROS, producing superoxide and hydrogen peroxide, respectively [4–7]. The role of NOX1 could be particularly important in the colon where the expression is highest [8–13], with an increasing expression gradient from proximal to distal end [9,10,13,14]. To convert oxygen to superoxide, NOX1 is dependent on a stabilizing protein ($p22^{phox}$), an activator (NOXA1), an organizer ($NOXO1/p47^{phox}$), and a Rac GTPase [4]. Colonic NOX1 is suggested to produce a basal level of ROS in the colon [4,15], which could be further enhanced during specific circumstances like inflammation [16] and bacterial invasion [15]. Another relevant RNS-producing enzyme in the intestine, not belonging to the NOX family, is inducible nitric oxide synthase (iNOS). iNOS produces nitric oxide which can spontaneously create peroxynitrite when reacting with superoxide [17]. While the expression of iNOS is high in the small intestine during normal conditions [18,19],

* Corresponding author.
E-mail addresses: anne.mari.herfindal@nmbu.no (A.M. Herfindal), sergio.rocha@nmbu.no (S.D.C. Rocha), dimitrios.papoutsis@nmbu.no (D. Papoutsis), siv.kjolsrud.bohn@nmbu.no (S.K. Bøhn), harald.carlsen@nmbu.no (H. Carlsen).

https://doi.org/10.1016/j.freeradbiomed.2022.06.234
Received 11 May 2022; Received in revised form 13 June 2022; Accepted 19 June 2022
Available online 23 June 2022

colonic iNOS is mainly expressed during inflammation or infection [20]. During inflammation, NOX2 in phagocytic cells will also contribute significantly to ROS/RNS generation [4].

The role of NOX1 in the colon is not fully understood. Still, studies of NOX1 have indicated its involvement in several processes, including endoplasmic reticulum stress in goblet cells [21], mucosal wound repair [16,22,23], and epithelial cell proliferation and differentiation [24]. NOX1 has also been proposed to be an important participant in crosstalk between the gut bacteria and the host [25,26]. Induced NOX1 mRNA expression in the colon of specific pathogen-free compared to germ-free mice [13] further indicates a relationship between colonic NOX1 and gut bacteria, although this result was not observed by others [19]. Together, these findings suggest important roles of NOX1 in colonic homeostasis. We have previously shown that NOX1 impacts bacterial levels and composition in the ileum [8], possibly through mechanisms involving NOX1- and iNOS-dependent formation of peroxynitrite, as assessed by *in vivo* and *ex vivo* imaging using the chemiluminescent molecule L-012 [8,27]. Similar mechanisms could be present in the colon during inflammation when both NOX1 and iNOS are active. Previous studies of NOX1's role during colon inflammation have mostly used pathological concentrations of dextran sulfate sodium (DSS; 2–4% in drinking water) [16,21,22,28], a widely used inducer of colitis. In those studies, NOX1-deficient mice exhibited overall small differences in colitis pathology compared to wild type (WT) mice. However, WT mice recover faster after the withdrawal of DSS [16] in line with NOX1's beneficial role in wound healing [22,23].

Severe colitis is an extreme situation with a massive release of inflammatory mediators and high production of ROS/RNS from many sources, which may mask the effects of the absence or presence of NOX1 in the DSS models using high concentrations. Thus, a more relevant condition for studying effects of NOX1 is low-grade colon inflammation, characterized by mild signs of inflammation with few or no signs of pathology [29], which can lead to impaired gut barrier integrity and disturbances in the bacterial composition of the colon. Low-grade intestinal inflammation is a state frequently encountered in patients with irritable bowel syndrome, in patients with inflammatory bowel disease in remission, and in people with a poor diet [29–33]. Low-grade inflammation can be induced in mice by applying low doses of DSS typically in the range of 0.5–1% [34]. Under these conditions, elevated levels of nitrotyrosine have been observed in the epithelial layers of the colon, indicative of enhanced peroxynitrite production [35], most likely facilitated by NOX1- and iNOS-dependent ROS/RNS formation. Since NOX1 is highly expressed in the colonic epithelial cells in healthy mice, it is plausible that NOX1 together with iNOS are the primary sources of peroxynitrite during low-grade inflammation induced by 1% DSS, and we speculate that in this condition peroxynitrite will have an impact on colon inflammation and bacterial composition.

The aim of this study was therefore to investigate the role of NOX1-dependent ROS/RNS production in the colon both during steady-state and during a mild and subclinical low-grade inflammation. Specifically, we wanted to investigate (1) whether ROS/RNS production in the colon is dependent on NOX1, (2) whether NOX1 has a protective role during low-grade colon inflammation, and (3) whether and how NOX1 impacts the bacterial composition in the colon.

2. Material and methods

2.1. Mice

All mice had C57BL/6J genetic background (The Jackson Laboratory, Bar Harbor, ME). NOX1 knockout (KO) mice (Jax stock #018787) [85] were bred by homozygous breeding ($Nox1^{-/-} \times Nox1^{-/Y}$) and the genotype was confirmed by standard PCR with specific primer pairs as recommended by The Jackson Laboratory (Table S1). WT and NOX1 KO mice were bred and housed in separate individually ventilated cages (Innovative, San Diego, CA) in the same controlled environment (rack) (12h-light-dark cycle, 24 ± 1°C, 45–55% humidity), with standard rodent chow (RM1, SDS Diet, Essex, UK) and water *ad libitum*. A low number of mice per cage (2–3) was maintained to reduce potential cage effects. Prior to the experiments, both genotypes were bred for several generations in the same rack with identical feeding and handling routines, thereby giving them the same external bacterial exposures.

2.2. Mouse experiments

Two mouse experiments were performed (Fig. 1). In Experiment 1, mice were treated with different doses of DSS in drinking water to find the optimal dose and length of DSS treatment to induce low-grade inflammation in the colon. In the present study, colonic low-grade inflammation refers to the presence of few or no visible signs of disease (i.e., weight loss and change in stool quality) together with a moderate up-regulation of inflammation-related genes. For this purpose, 24 WT male mice (10–14 weeks old) were divided into four groups (n=6) which were given 0, 0.5, 1 or 2% (w/w) DSS (Dextran Sulfate Sodium Salt Colitis Grade, 36,000–50,000 MW, MP Biomedicals, Santa Ana, CA) in water for eight days. In Experiment 2, WT and NOX1 KO mice were used to investigate the effect of NOX1-deficiency on ROS/RNS production, gut microbiota, and colonic low-grade inflammation. Nineteen WT and 20 NOX1 KO mice (14–17 weeks old) were used for this purpose. Mice of each genotype were divided into two groups (n=9–10, two males per group), each of which were given 0 or 1% (w/w) DSS in water for six days. For both experiments, fresh DSS solutions in new bottles were prepared every second day as recommended [36]. Water for the control mice was changed accordingly. Animal experiments were performed with permission from The Norwegian Food Safety Authority (FOTS #14805), and they were conducted in compliance with the current guidelines of The Federation of European Laboratory Animal Science Associations.

2.3. Sampling

Mice were weighed and stool quality was inspected every second day of the experiments. On the last day of the experiments, prior to termination, feces was collected for enzyme-linked immunosorbent assay (ELISA). Mice were then anesthetized by intraperitoneal injection with ZRF cocktail (10 μL/g mouse, Table S2). The feed was removed ~4 h before the ZRF injection. Blood for ELISA was collected through cardiac

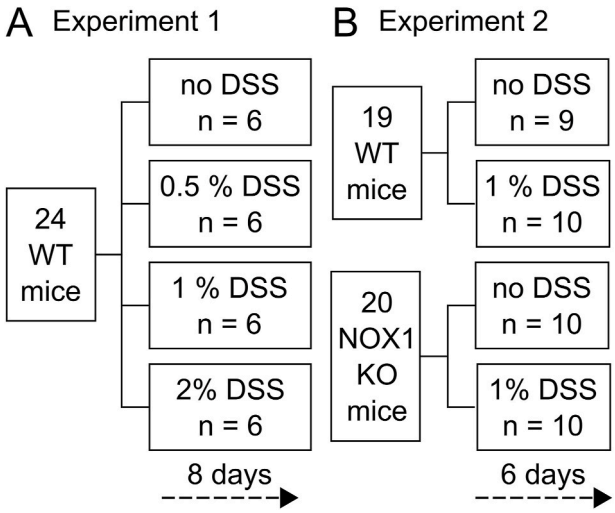

Fig. 1. Experimental group design for (A) Experiment 1 and (B) Experiment 2. In Experiment 1, WT mice were treated with 0 (no DSS), 0.5, 1, or 2% DSS for eight days (n=6 per group). In Experiment 2, WT and NOX1 KO mice were treated with 0 (no DSS) or 1% DSS for six days (n=9–10 per group). WT, wild type; DSS, dextran sulfate sodium; NOX1, NADPH oxidase 1; KO, knockout.

puncture with syringes coated with disodium EDTA as anticoagulant (0.05 M, final concentration 2–5 mM). After termination by cervical dislocation, the intestine was isolated and *ex vivo* imaging was performed (Experiment 2 only). After measuring the colon length, the colon was opened longitudinally, 2 cm from both sides. From these sections, 10–30 mg of lamina propria was scraped off with a glass slide for RNA extraction. The remaining middle segment was fixed for histological observations. In addition, 1 cm of the colon (referred to as "colon tissue") and one fecal pellet were collected from the proximal-middle section for DNA extraction (Experiment 2 only).

2.4. Ex vivo imaging of ROS/RNS using L-012 luminescence probe

Ex vivo imaging of the intestine in Experiment 2 was performed with IVIS Lumina II (PerkinElmer, Waltham, MA). On the termination day, L-012 luminescence probe (Wako Chemical, Neuss, Germany) was injected intraperitoneally (10 mg/kg mouse) after the ZRF injection. Light emission from intestine was measured as photons/second/cm^2/steradian 3 min after the L-012 injection with 5 min exposure time using the Living Imaging software (PerkinElmer). While presented images show both the small intestine and the colon, only the light emission from the colon was of interest and used for statistical analyses.

2.5. Quantification of LBP in plasma and LCN2 in feces using ELISA

ELISA was performed on plasma and feces from Experiment 2. Blood samples with disodium EDTA were placed on ice immediately after sampling. After centrifugation (10 min, 6000×*g*), plasma was collected and stored at −20°C until further processing. Plasma levels of lipopolysaccharide (LPS) binding protein (LBP) as a surrogate marker for LPS [37] were measured with Mouse LBP Quantification ELISA kit (Biometric, Greifswald, Germany) after diluting the plasma samples 800 times. After sampling, feces was stored at −80°C until further processing. Levels of lipocalin 2 protein (LCN2) in feces were used as an indicator of DSS-induced colon inflammation. Mouse Lipocalin-2/NGAL DuoSet ELISA and DuoSet ELISA Ancillary Reagent Kit 2 (R&D Systems, Minneapolis, MN) were used following the manufacturer's protocol. Feces was processed as described by Chassaing et al. [34] and supernatants were diluted between 20 and 20,000 times prior to the assay procedure. For both assays, levels of target protein were estimated using standard curves created using 4-parameter logistic curve fit and samples were analyzed in duplicates.

2.6. Histology

Histological analyses were performed on colon tissue from three mice per group from Experiment 2. Colon segments were fixed as a *swiss-roll* [38]. Briefly, the colon lumen was washed out with modified Bouin's fixative (50% ethanol, 5% acetic acid in dH_2O) and opened longitudinally. Segments were rolled into *swiss-roll* arrangement, with the luminal side facing inwards. Samples were kept in 10% buffered formalin overnight at room temperature and then stored in 70% ethanol at 4°C until standard ethanol dehydration procedures and paraffin embedding. Samples were cut with 7 μm thickness and stained with hematoxylin and eosin to be analyzed under an optical light microscope. The histological evaluation was based on the infiltration of immune cells in the lamina propria, space between epithelial cells bases and muscularis mucosa, and crypt structure, parameters commonly observed during DSS-induced colon inflammation [16,36].

2.7. RNA isolation and mRNA expression analyses of lamina propria

Lamina propria samples were placed in RNAlater (Sigma-Aldrich, St. Louis, MO) directly after sampling, stored at 4°C for 24 h, and then stored at −20°C until further processing. For RNA extraction, NucleoSpin RNA/Protein Purification kit (Macherey-Nagel, Düren, Germany) was used. DSS is known to inhibit both reverse transcriptase and PCR reactions [39,40]. Extracted RNA was therefore cleaned following the lithium chloride method as recommended [40]. Reverse transcriptase conversion of cleaned RNA to cDNA was performed using iScript cDNA Synthesis kit (Bio-Rad, Hercules, CA). For the qPCR reactions, we used HOT FirePol EvaGreen qPCR Supermix (Solis BioDyne, Tartu, Estonia) and measured fluorescence in LightCycler 480 Instrument II (Roche, Basel, Switzerland). Samples were analyzed in duplicates. LinRegPCR Software (version 2018.0) [41] was used to calculate quantification cycle (Cq) values based on a common threshold for all primers and individual primer efficiencies. The following target genes (*symbol*) were assessed: Tumor necrosis factor alpha (*Tnfa*), interleukin 6 (*Il6*), prostaglandin-endoperoxide synthase 2 (*Ptgs2*), interleukin 1 beta (*Il1b*), lipocalin 2 (*Lcn2*), cytochrome *b*-245 (*Cybb*, also known as *Nox2*), dual oxidase 2 (*Duox2*), inducible nitric oxide synthase 2 (*Nos2*, also known as *iNOS*), and NADPH oxidase 1 (*Nox1*, Experiment 1 only). The housekeeping gene glyceraldehyde-3-phosphate dehydrogenase (*Gapdh*) was used as reference, and relative mRNA expression for each target gene in each sample was calculated using the formula $R = (E_{target}{}^{(-Cq_{target})})/(E_{reference}{}^{(-Cq_{reference})})$ where E denotes the primer efficiency. See Tables S3–S7 for reagents, primers, and temperature cycles for cDNA synthesis and qPCR. Results are only presented for proximal colon.

2.8. DNA extraction from feces and colon tissue

Fecal pellets (~0.05 g) and colon tissue from Experiment 2 were placed in S.T.A.R buffer (300 μL, Roche) with acid-washed glass beads (app. 0.2 g, <106 m, Sigma-Aldrich) directly after sampling and stored at −80°C until further processing. Later, the fecal samples were added an additional 300 μL S.T.A.R buffer to obtain the same volumes (600 μL) as used during method testing. All samples were processed twice on FastPrep 96 (1800 rpm, 40 s, 5 min cooling step in-between, MP BioMedicals, Irvine, CA) to obtain cell lysis. Processed samples were centrifuged (~13,226×*g*, 10 min) and 50 μL supernatants were transferred to 96-well plates for protease treatment followed by DNA extraction using Mag Midi LGC kit (LGC Genomics, Teddington, UK) according to the manufacturer's protocol on a KingFisher Flex DNA extraction robot (Thermo Fisher Scientific, Waltham, MA).

2.9. Library preparation and gene sequencing of 16S rRNA

A similar workflow of 16S rRNA gene sequencing has been reported by others [42]. After DNA extraction, 16S rRNA genes were amplified by PCR using prokaryote-targeting primers (target region V3–V4, Table S8&S9). As DSS in feces has inhibitory effects on PCR (identified through dilution series on qPCR), we diluted the extracted DNA from fecal samples 1:4 prior to amplicon PCR (total dilution of 1:100 in PCR reaction). PCR products (~466 bp) were purified with AMPure XP (Beckman-Coulter, Indianapolis, IN) and 10 further PCR cycles with index primers modified with Illumina adapters were performed (Tables S10–S12), resulting in PCR products of ~594 bp. All PCR products were qualitatively confirmed by gel electrophoresis. Quantification, normalization, and pooling of individual libraries were followed by purification by AMPure XP and quantification of the pooled library. The pooled library was diluted to 6 pM and sequenced with the MiSeq Reagent Kit V3 (cat. nr. MS-102-3003, Illumina, San Diego, CA) on the Illumina MiSeq following Illumina's protocol (16S Metagenomic Sequencing Library Preparation Part# 15044223 Rev. B), except we used nuclease free-water instead of Tris for PhiX library dilution. 20% PhiX served as an internal control.

2.10. Processing of 16S rRNA gene sequencing data

The resulting 300 bp paired-end reads from gene sequencing of 16S

rRNA were paired-end joined and split into their respective samples, quality-filtered using QIIME [43], and clustered into taxonomically assigned operational taxonomic units (OTUs) with ≥97% identity using closed-reference *usearch* algorithm (version 8) [44,45] against the SILVA database (version 128) [46]. The resulting dataset included 2,392,173 high-quality and chimera-checked sequences from the 78 samples (8644 to 61,079 sequences/sample). The OTU counts for each sample were normalized by even subsampling (rarefaction) in QIIME with 6500 sequences per sample as normalization cut-off. In the normalized dataset, 538 OTUs were identified in total (rarefaction curves in Fig. S1). The OTUs were taxonomically binned into phylum- and genus-level abundance tables. Abundances of bacterial taxa are presented as relative abundances (%) where the lowest detectable abundance was 0.015%.

2.11. Alpha- and beta-diversity

Measures of bacterial diversity within (α-diversity; number of observed species, Shannon-Wiener index, and evenness) and between (β-diversity; Bray-Curtis and weighted UniFrac distances [47]) samples were calculated based on the normalized OTU table.

The number of observed species in one sample was calculated as the number of OTUs with sequence count >0. The Shannon-Wiener index for one sample was calculated as $H = -\sum_{i=1}^{s}(p_i ln(p_i))$, where s denotes the number of OTUs with sequence count >0 and p_i the proportion of the community represented by OTU number i. Equitability (evenness) for one sample was calculated as $E = H/H_{max}$ where $H_{max} = \ln(\text{number of OTUs with sequence count} > 0)$.

β-diversities (Bray-Curtis and weighted UniFrac distances) between samples were calculated using QIIME default scripts (core_diversity_analyses.py). Analyses of β-diversities were conducted in R [48] (version 4.1.2). Ordination of β-diversities by non-metric multidimensional scaling (NMDS) was performed using the metaMDS() function from the *vegan* package [49] (version 2.5–7), with autotransform=FALSE and try=100. Ordination of β-diversities by principal coordinate analyses (PCoA) was performed using the cmdscale () function from the *stats* package [48] (version 4.1.2) with k=2. Global PERMANOVA of β-diversities was performed using the adonis() function from the *vegan* package with permutations=999, p.method="BH", and nperm=999 (four groups: WT, WT + 1% DSS, NOX1 KO, and NOX1 KO + 1% DSS). Dispersion homogeneity between groups was assessed using the function betadisper() from the *vegan* package. Significant global PERMANOVA was followed by pairwise PERMANOVA, performed by applying the pairwise.perm.manova() function from the *RVAideMemoire* package (version 0.9–79) [50] with nperm=999 and p.method="BH". The p-values reported from global and pairwise PERMANOVA are the mean p-values from 100 PERMANOVA runs. PERMANOVA was performed separately for feces and colon tissue.

2.12. Statistics

All statistical analyses, except PERMANOVA (section 2.11) and linear discriminant analysis (LDA) effect size (LEfSe), were performed using GraphPad Prism (version 9.3.0 for Windows, GraphPad Software, San Diego, California USA). All reported p-values are two-tailed where $p<0.05$ was considered significant.

Colon length and mRNA expression data from Experiment 1 (0, 0.5, 1 and 2% DSS in WT mice) were analyzed using one-way ANOVA while body weight change was analyzed using repeated measures 2-way ANOVA. Significant effect of DSS in one-way ANOVA was followed by pairwise comparison of the four different DSS doses using Tukey's test for multiple comparisons. Significant effect of day and DSS dose in the repeated measures 2-way ANOVA was followed by pairwise comparison of DSS doses within each day using Tukey's test for multiple comparisons. mRNA expression data were log10-transformed to obtain normally distributed model residuals with equal residual variance between groups.

Colon length, L-012 signal, mRNA expression, protein biomarkers, α-diversity, and phylum abundance data from Experiment 2 (effects of 1% DSS treatment and genotype) were analyzed using 2-way ANOVA when appropriate while body weight change was analyzed using repeated measures 3-way ANOVA. Significant interactions between treatment and genotype in 2-way ANOVA were followed by the assessment of simple main effects (effect of treatment within each genotype and effect of genotype within each treatment) with Bonferroni correction for multiple comparisons. mRNA expression, protein biomarkers, and some phylum abundance data (specified in figure captions) were log10-transformed to obtain normally distributed model residuals with equal residual variance between groups. In cases where residuals from 2-way ANOVA were not reasonably normally distributed or when equality of residual variance between groups could not be reasonably assumed (even after data transformation), comparisons of genotypes (WT versus NOX1 KO) were performed within each treatment (0 and 1% DSS) using a model suitable for each case (*t*-test, Welch's *t*-test, Mann-Whitney test, or Fisher's exact test, specified in figure captions).

Normality of model residuals was evaluated using Q-Q plot and Shapiro-Wilk test and homoscedasticity of model residuals was evaluated using residual plots and Brown-Forsythe test. Data are presented as individual values (with some exceptions) with group means ± standard error of the mean (SEM) or geometric group mean ×/÷ geometric SD factor in cases where statistical analyses were performed on log10-transformed data.

To identify differentiated bacterial genera between groups, we used LEfSe [51] available at https://huttenhower.sph.harvard.edu/galaxy/, with $p<0.05$ and the LDA effect size 2.0 to explain differences between groups.

3. Results

3.1. Establishment of the low-grade colon inflammation model

The main aim of the study was to investigate the role of NOX1-dependent ROS/RNS production in the colon during steady-state and DSS-induced low-grade colon inflammation. The criteria set for a relevant inflammation model were few or no visible signs of disease together with a moderate up-regulation of inflammation-related genes in the colonic mucosa. To find the optimal time-dose for inducing low-grade colon inflammation, we treated WT mice with 0, 0.5, 1, or 2% DSS for eight days (Experiment 1).

Mice treated with the highest dose of 2% DSS had significant weight loss after six days (Fig. S2A). Mice treated with 0.5 or 1% DSS showed only marginal or no weight loss and did not differ significantly from untreated mice. From day four, 2% DSS-treated mice presented poorer stool quality i.e., loose consistency and traces of blood, while 1 and 0.5% DSS-treated mice only presented minor changes by day six and eight, respectively. At termination (day eight), 2% DSS-treated mice had significantly shorter colons than all other groups, whereas the colon length of 0.5 and 1% DSS-treated mice were not different from untreated mice (Fig. S2B).

Compared to untreated mice, DSS-treated groups had a dose-dependent higher mRNA expression of the inflammation-related genes *Tnfa*, *Ptgs2*, *Il6*, *Il1b*, and *Lcn2*, and of the ROS/RNS-related genes *Nox2*, *Duox2*, and *iNOS* in the colonic mucosa at termination (Figs. S3A–H). The lowest dose of 0.5% DSS was not associated with higher expression of the inflammation- or ROS/RNS-related genes, except for *Tnfa*. Expression of *Nox1* was unaffected by all DSS doses tested (Fig. S3I).

Based on the results from Experiment 1, we concluded that treatment with 1% DSS for six days would be a suitable dose and duration to induce low-grade colon inflammation due to lack of marked clinical signs while high enough to significantly up-regulate inflammation- and relevant ROS/RNS-related genes.

3.2. NOX1 is important for ROS/RNS production in the colon

For the main experiment, where WT and NOX1 KO mice were treated with 0 or 1% DSS for six days (Experiment 2), we first sought to investigate whether the colonic ROS/RNS production was dependent on NOX1, especially during DSS-induced inflammation. We hypothesized that the ROS/RNS levels in NOX1 KO mice would be significantly lower than in WT mice, mainly due to lack of NOX1-dependent peroxynitrite formation.

L-012 luminescence from *ex vivo* imaging of the colons at termination (day six) was used as a sensor of ROS/RNS (Fig. 2A&B). Regardless of genotype, the L-012 mediated ROS/RNS signal was higher in DSS-treated mice than in untreated mice. Furthermore, in agreement with our hypothesis, the ROS/RNS signal was significantly lower in NOX1 KO than in WT mice, both with and without DSS treatment. In untreated and DSS-treated mice, the average (median) ROS/RNS signal in WT mice was ~2 and ~5 times higher, respectively, than in NOX1 KO mice.

Next, we investigated the importance of the ROS/RNS-related genes *iNOS*, *Duox2*, and *Nox2* for the ROS/RNS production by assessing the mRNA expression in the colonic mucosa at termination. All these genes encode enzymes which can contribute to the L-012 signal (i.e., ROS/RNS production) through different reaction pathways. Expression of *iNOS* was higher in DSS-treated than in untreated mice, but no difference was found between WT and NOX1 KO mice (Fig. 2C). *Duox2* expression was only moderately elevated in DSS-treated mice with no differences between WT and NOX1 KO mice (Fig. 2D) while expression of *Nox2* was unaffected by both DSS treatment and genotype (Fig. 2E). The median expression of *iNOS* and *Duox2* was about 40 and 2 times higher, respectively, in DSS-treated compared to untreated mice.

Taken together, these data show that NOX1-deficiency abolished ROS/RNS-dependent L-012 luminescence despite DSS-induced high expression of both *iNOS* and *Duox2*. Additionally, we show that expression of *iNOS* and *Duox2* was not dependent on NOX1.

3.3. NOX1 has minor impact on the susceptibility for DSS-induced low-grade colon inflammation

Since *ex vivo* imaging with L-012 indicated reduced ROS/RNS production in the NOX1 KO mice, we next asked whether the lack of NOX1-dependent ROS/RNS would affect the severity of the 1% DSS-induced low-grade colon inflammation. We hypothesized that NOX1 would have a protective role where NOX1 KO mice would be more susceptible to inflammation.

Six days of 1% DSS treatment did not result in significant changes in body weight for WT or NOX1 KO mice (Fig. S4A). Most of the DSS-treated mice displayed changes in stool quality from day four and they had reduced colon length at termination compared to untreated mice, but these changes were not different between WT and NOX1 KO mice (Fig. S4B).

To further evaluate the severity of the inflammation, we measured the mRNA expression of the inflammation-related genes *Tnfa*, *Il6*, *Ptgs2*, *Il1b*, and *Lcn2* in the colonic mucosa at termination. All genes were significantly higher expressed in DSS-treated than in untreated mice (Fig. 3A–E). Further, for *Tnfa*, there was a significant interaction

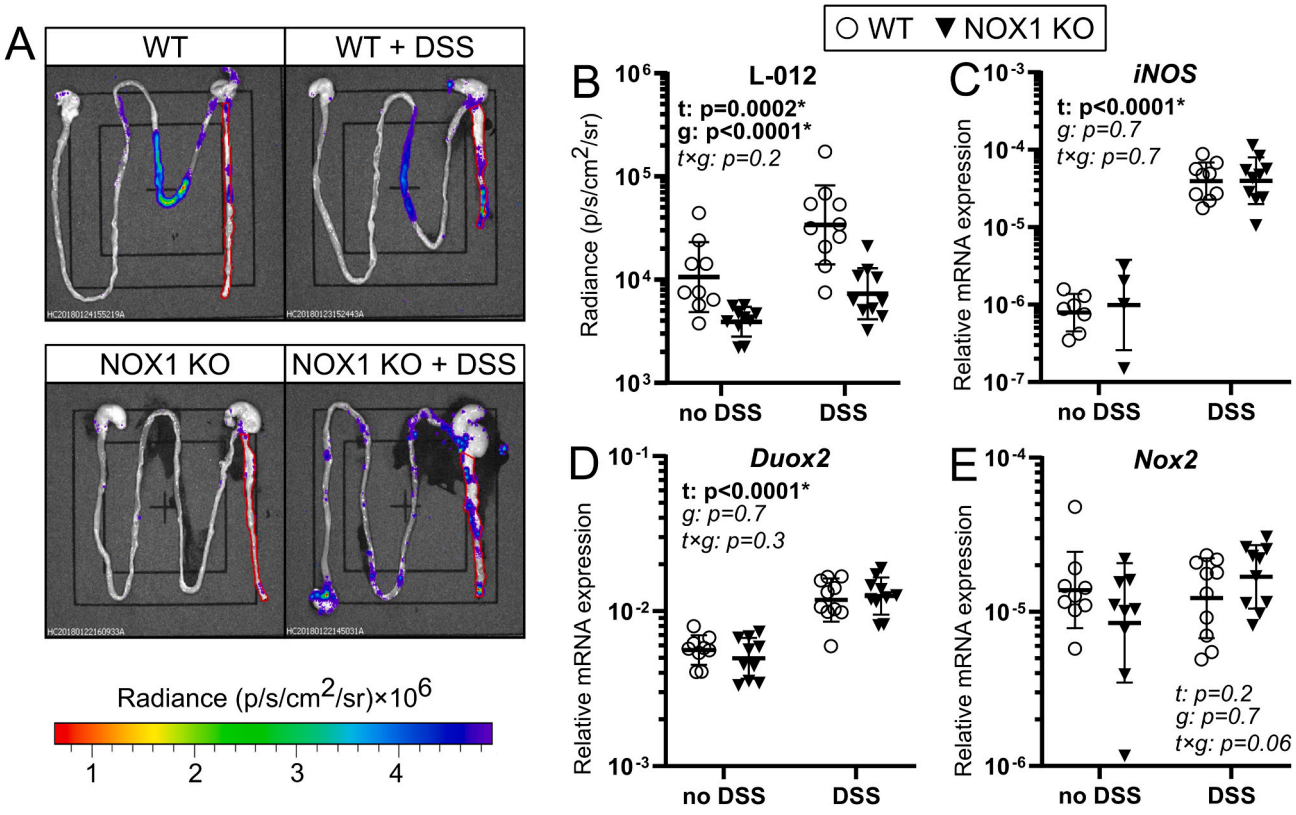

Fig. 2. ROS/RNS production in the colon of WT and NOX1 KO mice with or without 1% DSS treatment for six days. (A) Representative *ex vivo* images of one animal from each of the four groups after injection with L-012. Pseudo colors represent light intensity expressed as photons/sec/cm^2/steradian (p/s/cm^2/sr). Red markings show the region of interest (ROI) in the colon. (B) L-012-induced chemiluminescence from the colon ROI expressed as average radiance (p/s/cm^2/sr). n=9–10 per group. (C–E) Relative mRNA expression of (C) inducible nitric oxide synthase 2 (*iNOS*) (D), dual oxidase 2 (*Duox2*), and (E) cytochrome *b*-245 (*Nox2*) in mucosa from the proximal colon. n=4–10 per group. P-values from 2-way ANOVA (main effect of treatment (t; no DSS versus 1% DSS) and genotype (g; WT versus NOX1 KO), and interaction effect (t×g)) on log10-transformed data. Horizontal lines and whiskers are geometric group mean ×/÷ geometric SD factor. ROS, reactive oxygen species; RNS, reactive nitrogen species, WT, wild type; NOX1, NADPH oxidase 1; KO, knockout; DSS, dextran sulfate sodium. *p<0.05. (For interpretation of the references to color in this figure legend, the reader is referred to the Web version of this article.)

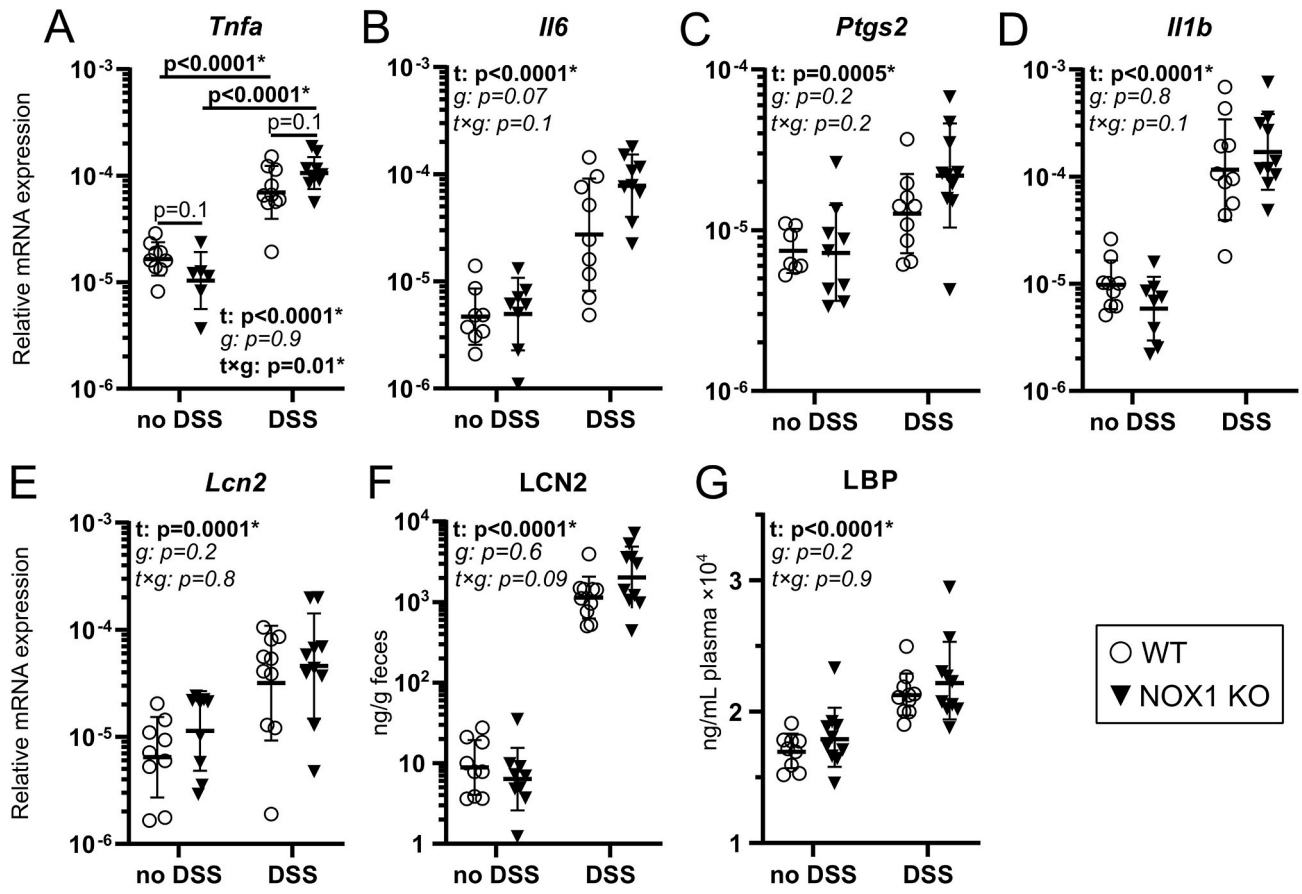

Fig. 3. Mucosal inflammation and intestinal barrier integrity of WT and NOX1 KO mice with or without 1% DSS treatment (6 days). (A–E) Relative mRNA expression of (A) tumor necrosis factor alpha (*Tnfa*), (B) interleukin 6 (*Il6*), (C) prostaglandin-endoperoxide synthase 2 (*Ptgs2*), (D) interleukin 1 beta (*Il1b*), and (E) lipocalin 2 (*Lcn2*) in mucosa from the proximal colon. n=6–10 per group. (F) Concentration of fecal lipocalin 2 protein (LCN2). n=9–10 per group. (G) Concentration of lipopolysaccharide binding protein (LBP) in plasma. n=9–10 per group. P-values from 2-way ANOVA (main effect of treatment (t; no DSS versus 1% DSS) and genotype (g; WT versus NOX1 KO), and interaction effect (t×g)) on log10-transformed data. In cases with significant interaction, p-values for simple main effects from post-hoc tests with Bonferroni correction for multiple comparisons are presented. Horizontal lines and whiskers are geometric group mean ×/÷ geometric SD factor. WT, wild type; NOX1, NADPH oxidase 1; KO, knockout; DSS, dextran sulfate sodium. *p<0.05.

between treatment and genotype, indicating a stronger DSS-induced up-regulation of *Tnfa* in NOX1 KO than in WT mice (Fig. 3A). Similar trends were observed for *Il6* (Fig. 3B) and *Ptgs2* (Fig. 3C).

In addition to mRNA expression, we also investigated if the protein levels of LCN2 in feces were different between DSS-treated WT and NOX1 mice, as fecal LCN2 has been shown to be a sensitive marker of colon inflammation [34]. As for *Lcn2* mRNA expression, the LCN2 protein levels were higher in DSS-treated than in untreated mice. Furthermore, DSS-treated NOX1 KO mice tended to have higher LCN2 levels than DSS-treated WT mice, although not significantly (Fig. 3F). As a measure of intestinal barrier breach, commonly associated with colon inflammation, we also measured the protein levels of LBP in plasma. LBP levels were higher in DSS-treated than in untreated mice, but no differences were found between WT and NOX1 KO mice (Fig. 3G).

Finally, we evaluated the structural impacts of the DSS treatment on colon tissue in a selection of WT and NOX1 KO (n=3 per group). Both WT and NOX1 KO mice displayed similar mild signs of colon inflammation in response to DSS, with infiltration of immune cells in lamina propria and increased space between epithelial cell bases and muscularis mucosa (Fig. 4). In mice not treated with DSS, no signs of colon inflammation were observed in neither of the genotypes.

3.4. NOX1 affects the community structure and diversity of the colonic microbiota

To assess the role of NOX1 on the colonic microbiota both during steady-state and inflammatory conditions, we performed 16S rRNA gene sequencing of both feces and colon tissue samples, representing the luminal- and mucosa-associated microbiota, respectively.

First, two different measures of between-sample diversity (β-diversity) were used to assess the overall differences in bacterial community structures between the four groups of mice: 1) Bray-Curtis distances (based on OTU abundances) and 2) weighted UniFrac distances (abundance-weighted phylogenetic distances). As illustrated in NMDS ordination plots in Fig. 5A&C, feces samples clustered significantly according to both DSS treatment and genotype for both Bray-Curtis and weighted Unifrac distances, where all four groups were significantly different from each other. For colon tissue, we also found significant clustering according to both DSS treatment and genotype when applying Bray-Curtis distances (Fig. 5B) while for weighted Unifrac, samples clustered only according to treatment with no difference between WT and NOX1 KO mice (Fig. 5D). The same clustering patterns were obtained when applying PCoA as ordination method (Fig. S5).

We next examined the effect of NOX1 and DSS treatment on fecal bacterial diversity (richness and evenness) by applying three selected indices of within-sample diversity (α-diversity): 1) The Shannon-Wiener index (richness and evenness combined; Fig. 6A), 2) number of observed species (richness; Figs. 6B), and 3) evenness (Fig. 6C). Untreated NOX1 KO mice had lower diversity than untreated WT mice for all the three indices. Further, regardless of genotype, DSS-treated mice had higher Shannon-Wiener index and evenness compared to untreated mice, while number of observed species was unaffected by DSS treatment.

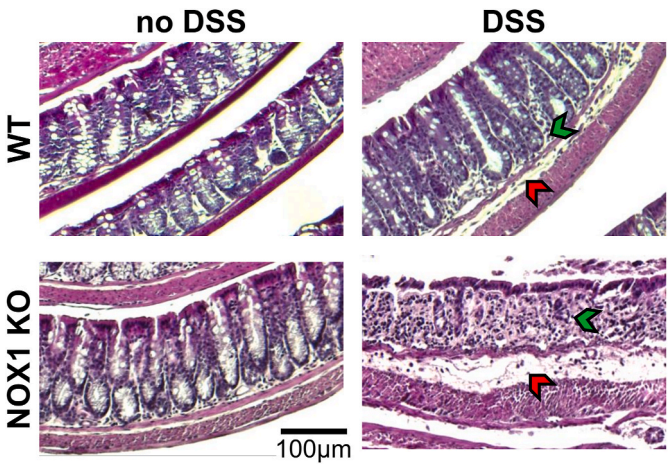

Fig. 4. Colon tissue of WT and NOX1 KO mice with or without 1% DSS treatment (6 days). Representative images (n=3 per group) except from DSS-treated NOX1 KO mouse. In this case we present the most severe observed case. The other DSS-treated NOX1 KO mice could not be distinguished from the DSS-treated WT mice. Green arrows indicate the infiltration of immune cells into the lamina propria. Red arrows indicate increased space between epithelial cell bases and muscularis mucosa. Colon sections (7 μm) were stained with hematoxylin and eosin. WT, wild type; NOX1, NADPH oxidase 1; KO, knockout; DSS, dextran sulfate sodium. (For interpretation of the references to color in this figure legend, the reader is referred to the Web version of this article.)

Interestingly, with DSS treatment, the difference in evenness between WT and NOX1 KO mice observed in untreated mice was no longer present. Similar patterns were found for colon tissue, although not as prominent (Fig. 6D–F).

In conclusion, the results on β- and α-diversity illustrate 1) that both NOX1 and DSS treatment highly affects the overall structures of the bacterial communities, 2) that NOX1 KO mice generally display a lower bacterial diversity than WT mice, and 3) that the differences between WT and NOX1 KO mice are more prominent for the luminal-associated microbiota.

3.5. NOX1 affects colonic bacterial composition at the phylum level

Based on the assessment of overall bacterial community structure and diversity, it was clear that the NOX1 KO and WT mice had considerable differences in the colonic microbiota, both during steady-state and inflammatory conditions. To obtain a more detailed understanding of these differences, we first assessed the effects of NOX1 and DSS treatment on the relative bacterial abundances at the phylum level (Fig. 7A). Only phyla with average relative abundance above 1% in at least one group were included in the analyses (individual plots for all analyzed phyla in Fig. S6).

In both feces and colon tissue, representing the luminal- and mucosa-associated microbiota, respectively, the main effects of DSS treatment were higher abundance of Firmicutes and Tenericutes, while lower abundance of Bacteroidetes and Proteobacteria. No main effect of genotype was found for any of the above-mentioned phyla. However, in feces, we found significant interaction between treatment and genotype for Bacteroidetes (Fig. 7B, Fig. S6B) and Firmicutes (Fig. 7C, Fig. S6A). Untreated NOX1 KO mice had lower abundance of Bacteroidetes than untreated WT mice, while there was no difference between the genotypes when treated with DSS, mainly due to reduced abundance in the WT mice. For Firmicutes, no significant differences were found between NOX1 KO and WT mice, but a tendency towards higher abundance in untreated NOX1 KO than in untreated WT mice. In addition to the higher Firmicutes/Bacteroidetes ratio in NOX1 KO mice, the phylum Verrucomicrobia was significantly more abundant in feces from NOX1 KO than from WT mice, both with and without DSS treatment (Fig. 7D, Fig. S6I). Furthermore, WT mice treated with DSS had higher abundance of Verrucomicrobia than untreated WT mice, but the levels were still lower than in NOX1 KO mice. The Verrucomicrobia abundance showed similar patterns in colon tissue.

3.6. NOX1 affects colonic bacterial composition at the genus level

To assess the effect of NOX1 and DSS treatment on the relative abundances at the genus level, we performed LEfSe separately for feces and colon tissue for the four relevant comparisons: comparison of genotypes (WT and NOX1 KO) within each treatment condition (0 and 1% DSS), and comparison of treatments within each genotype. From the LEfSe results (Figs. S7–S10), 21 genera in total were identified as different between NOX1 KO and WT mice in feces and/or colon tissue. Twelve LEfSe-identified genera were considered abundant (average abundance above 0.1% in feces and/or colon tissue, Fig. 8) while nine were low abundant (Fig. S11).

Of the abundant LEfSe-identified genera, *Lachnospiraceae FCS020 group* was the only one to be unaffected by DSS treatment itself and the abundance was generally lower in NOX1 KO than in WT mice (Fig. 8A). The genera *Faecalibaculum*, *Lachnospiraceae UCG-001*, and *unknown Bacteroidales S24-7 group* (identical to family *Bacteroidales S24-7 group*) had, with some exceptions, lower abundance in NOX1 KO than in WT mice and were decreased by DSS treatment in both genotypes (Fig. 8B–D). *Alistipes* (identical to family *Rikenellaceae*) was overall decreased by DSS, but more strongly in NOX1 KO mice, resulting in lower abundance of this genus in NOX1 KO mice compared to WT when treated with DSS (Fig. 8E). The abundance of *Akkermansia* (identical to phylum Verrucomicrobia, see section 3.5) was much higher in NOX1 KO mice compared to WT both in untreated and DSS-treated mice, and DSS led to enrichment of *Akkermansia* only in the WT mice (Fig. 8F). In untreated mice, *Oscillibacter* and *Ruminococcaceae UCG*-005 had similar abundances between WT and NOX1 KO mice, while DSS led to enrichment only in the NOX1 KO mice (Fig. 8G&H). Three genera *Ruminococcus1*, *unknown Peptococcaceae* and *unknown MollicutesRF9* (identical to order MollicutesRF9) showed an abundance pattern where DSS treatment led to enrichment, but only the WT mice (Fig. 8I–K). Finally, NOX1 KO mice had lower abundance of *Blautia* compared to WT when not treated with DSS, and while DSS treatment led to decreased levels in WT mice, *Blautia* was enriched in DSS-treated NOX1 KO mice (Fig. 8L).

Of the low abundant genera identified by LEfSe, two genera showed particularly distinct differences between NOX1 KO and WT mice. *Ruminiclostridium1* was only detected in NOX1 KO mice (Fig. S11A), while *Peptococcus* was almost exclusively found in WT mice (Fig. S11B).

4. Discussion

As a primary producer of ROS/RNS in colonic epithelial cells, NOX1 contributes to intestinal homeostasis [16,21–24] and its role could be particularly relevant when combined with other ROS/RNS-generating enzymes such as iNOS [8]. In this study, we hypothesized that NOX1-dependent ROS/RNS production influences the severity of low-grade inflammation and bacterial composition in the colon. To explore this hypothesis, we investigated the effects of NOX1-deficiency on ROS/RNS production, markers of inflammation, and bacterial composition in the colon both during steady-state and in 1% DSS-induced subclinical low-grade colon inflammation. While reduced levels of ROS/RNS in the colon of NOX1 KO mice only marginally aggravated the severity of inflammation, the colonic microbiota was highly affected by the lack of NOX1-depedent ROS/RNS.

As a marker of extracellular ROS/RNS in the colon, we used L-012, a chemiluminescent molecule that emits light when it reacts with various ROS/RNS, most prominently peroxynitrite, hypochlorous acid and hydroxyl radical [52–57]. While DSS treatment increased colonic ROS/RNS levels, the levels were substantially lower in NOX1 KO mice than in WT. Reduced L-012 signal in the colon of NOX1-deficient mice in

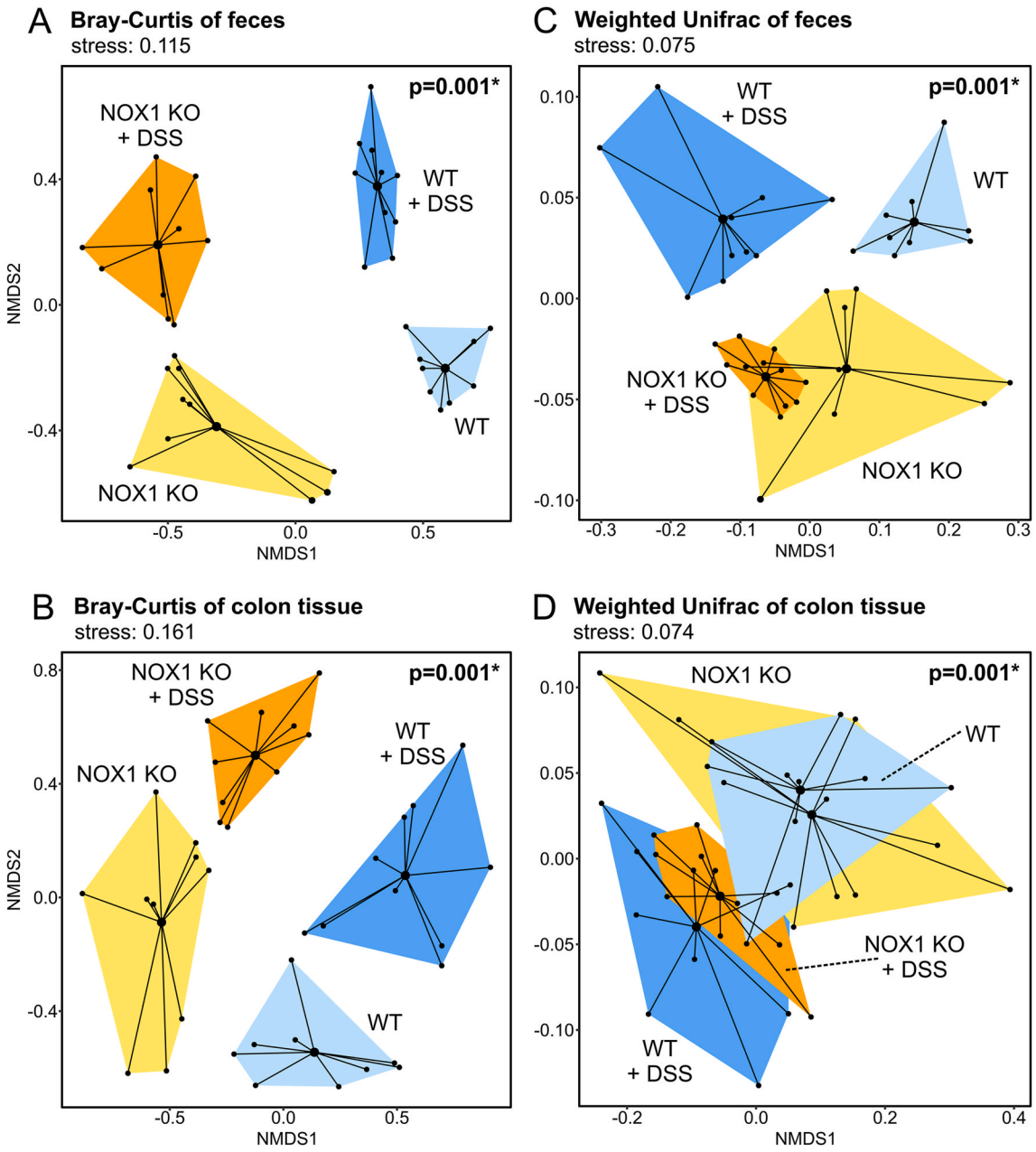

Fig. 5. Bacterial β-diversity between WT and NOX1 KO mice with or without 1% DSS treatment (6 days). NMDS ordination plots of (A,B) Bray-Curtis and (C,D) weighted UniFrac distances between (A,C) feces and (B,D) colon tissue samples. Colors indicate which group individual samples belong to. Stress values indicate the NMDS goodness-of-fit. n=9–10 per group. P-values in graph from global PERMANOVA. For data presented in A, B, and C, pairwise PERMANOVA showed a significant difference between all four groups (all $p \leq 0.007$). For data presented in D, there was no difference between genotypes in neither treatment condition (no DSS: all $p > 0.2$; DSS: all $p > 0.7$), only across treatment independent of genotype (all p's<0.03). WT, wild type; NOX1, NADPH oxidase 1; KO, knockout; DSS, dextran sulfate sodium; NMDS, non-metric multidimensional scaling. *$p<0.05$. (For interpretation of the references to color in this figure legend, the reader is referred to the Web version of this article.)

steady-state conditions has been reported by others [11,58], but we show here that NOX1 is also important for colonic ROS/RNS production during DSS-induced inflammation. Together with the marked DSS-induced up-regulation of *iNOS* mRNA, but not of *Nox1*, *Nox2*, or *Duox2*, our results suggest that the DSS-increased L-012 signal in WT mice originated primarily from peroxynitrite, formed by NOX1-and iNOS-dependent production of superoxide and nitric oxide, respectively. Still, although *Nox1* expression was not affected by DSS treatment, we cannot claim that iNOS alone was responsible for the increased L-012 signal, as colitis can cause increased protein expression [16] and enzyme activity [59] of NOX1. Further, since DSS also increased the L-012 signal in the absence of NOX1, although modestly, it appears that peroxynitrite was not the sole source of the L-012 signal. One possible explanation for this observation is that *Duox2,* which can give rise to hydroxyl radical and hypochlorous acid via hydrogen peroxide, was modestly up-regulated by DSS. The formation of hypochlorous acid from hydrogen peroxide is catalyzed by myeloperoxidase, which can be induced by 1% DSS [34]. Lastly, deletion of NOX1 may cause up-regulation of other NOXs such as NOX3 [28] as a compensatory mechanism that can also contribute to the ROS/RNS mediated L-012 signal.

Even though the ROS/RNS production was clearly reduced in NOX1 KO mice, these mice did not have higher susceptibility towards low-grade inflammation than WT with regard to crude inflammatory

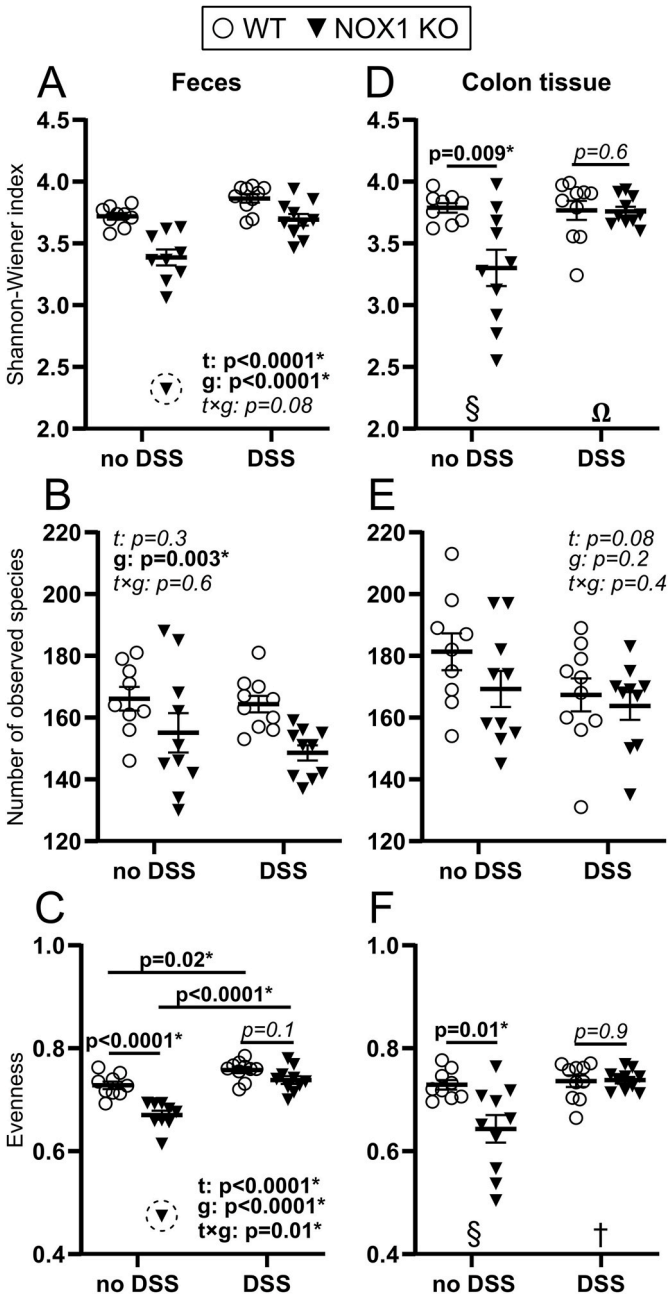

Fig. 6. Bacterial α-diversity in the colon of WT and NOX1 KO mice with or without 1% DSS treatment (6 days). (A,D) Shannon-Wiener index, (B,E) number of observed species (OTUs), and (C,F) evenness (equitability) of bacterial communities in (A–C) feces and (D–F) colon tissue. P-values from 2-way ANOVA (main effect of treatment (t; no DSS versus 1% DSS) and genotype (g; WT versus NOX1 KO), and interaction effect (t×g)). In cases with significant interaction, p-values for simple main effects from post-hoc tests with Bonferroni correction for multiple comparisons are presented. In two cases (A and C), extreme value was excluded from statistical analysis (dotted circles). When included, the significance of the interaction increased for the Shannon-Wiener index (p=0.06) and decreased for evenness (p=0.02). In cases where 2-way ANOVA could not be performed due to heteroskedasticity and/or violation of normality assumption alternative tests were used within the two treatment groups: (§) Welch's *t*-test, (Ω) Mann-Whitney test, or (†) *t*-test. n=9–10 per group. Horizontal lines and whiskers are group mean ± SEM. WT, wild type; NOX1, NADPH oxidase 1; KO, knockout; DSS, dextran sulfate sodium; OTU, operational taxonomic unit. *p<0.05.

disease markers evaluated by body weight, colon length, stool quality, and histology. These observations are in line with other studies of NOX1-deficient mice using higher DSS concentrations [21,28]. However, the lack of more pronounced inflammation in NOX1 KO mice could be attributed to a NOX3 compensatory mechanism [28], as alluded to above. Mice deficient of the enzyme NOXO1, the organizing subunit of NOX1 and NOX3 [4], display a stronger pathological response than WT mice during DSS-induced colitis [11]. Thus, in the absence of NOX1-generated superoxide, up-regulation of NOX3 may to some extent compensate for NOX1-loss.

Despite no differences between NOX1 and WT mice regarding crude signs of inflammation after DSS treatment, mRNA levels of genes encoding the pro-inflammatory mediators TNF-α, IL-6, and PTGS2 (COX2) tended to be higher in the colonic mucosa of NOX1 KO than of WT mice. In line with our results, Kato *et al.* demonstrated that NOX1 KO mice had higher COX2 expression than WT mice following DSS colitis during the restitution phase [16]. The concentration of fecal LCN2, a highly sensitive marker of colon inflammation [34] was also higher in NOX1 KO than in WT mice. Collectively, these findings indicate a slightly elevated susceptibility to DSS-induced low-grade inflammation in NOX1-deficient mice. Since LCN2 expression is dependent on bacterial exposure [60], we speculate that the absence of NOX1 weakens the epithelial barrier, resulting in closer contact between the colonic bacteria and epithelial cells which again can result in compromised epithelial layer and more LCN2 in the lumen. NOX1-generated ROS has been implicated in cytoprotection in epithelial cells, mediated through the redox-sensitive transcription factor Nrf2 [61]. Impaired barrier function in NOX1-deficient mice could therefore be related to the inability to withstand the stress imposed by DSS treatment. That Nrf2 is important for protection against DSS-induced colitis has been demonstrated previously [62], possibly by inhibiting NF-κB activation [63]. Additionally, the absence of NOX1-generated superoxide could lead to altered bacterial composition in the colon, analogous to observations of the ileum [8] with implications for LCN2 expression. Indeed, Li and coworkers showed that DSS-induced LCN2 levels were dependent on the initial gut microbiota profile [64].

Regarding the colonic microbiota, our initial hypothesis was that NOX1-dependent extracellular ROS/RNS, particularly peroxynitrite, could act as bactericidal molecules affecting the colonic microbiota, and that this effect would be most prominent during DSS-induced inflammation due to marked up-regulation of iNOS. However, the results from 16S sequencing show that the WT and NOX1 KO mice had large differences in bacterial composition both with and without DSS treatment, indicating that peroxynitrite is not decisive for NOX1-dependent changes in the microbiota. NOX1-deficiency may affect the microbiota during steady-state through more indirect effects including NOX1-dependent signaling in epithelial cells that could affect goblet cell abundance and the mucus layer [16,24].

Specifically, we found that the colonic microbiota of NOX1-deficient mice was characterized by lower fecal α-diversity and changes in the relative abundance of specific bacterial taxa. Analogously, others have demonstrated that pharmacological removal of luminal ROS/RNS in the colon can lead to decreased bacterial diversity [65], indicative of a less stable community more vulnerable to perturbations [66]. When focusing on the relative abundance of individual bacterial taxa, a general pattern was that DSS-untreated NOX1 KO mice had abundance shifts resembling those induced by DSS treatment in WT mice, characterized mainly by a higher abundance of Firmicutes and Verrucomicrobia (genus *Akkermansia*), and lower abundance of Bacteroidetes (mainly family *Bacteroidales S24-7 group*). When treated with DSS, the most striking differences between the genotypes were the higher and lower abundances of *Oscillibacter* and *Alistipes*, respectively, in NOX1 KO mice. Low abundance of both S24-7 and *Alistipes* has been found to correlate with higher levels of pro-inflammatory cytokines [67], and *Alistipes* has been suggested to have a protective role in DSS-induced colitis [67,68].

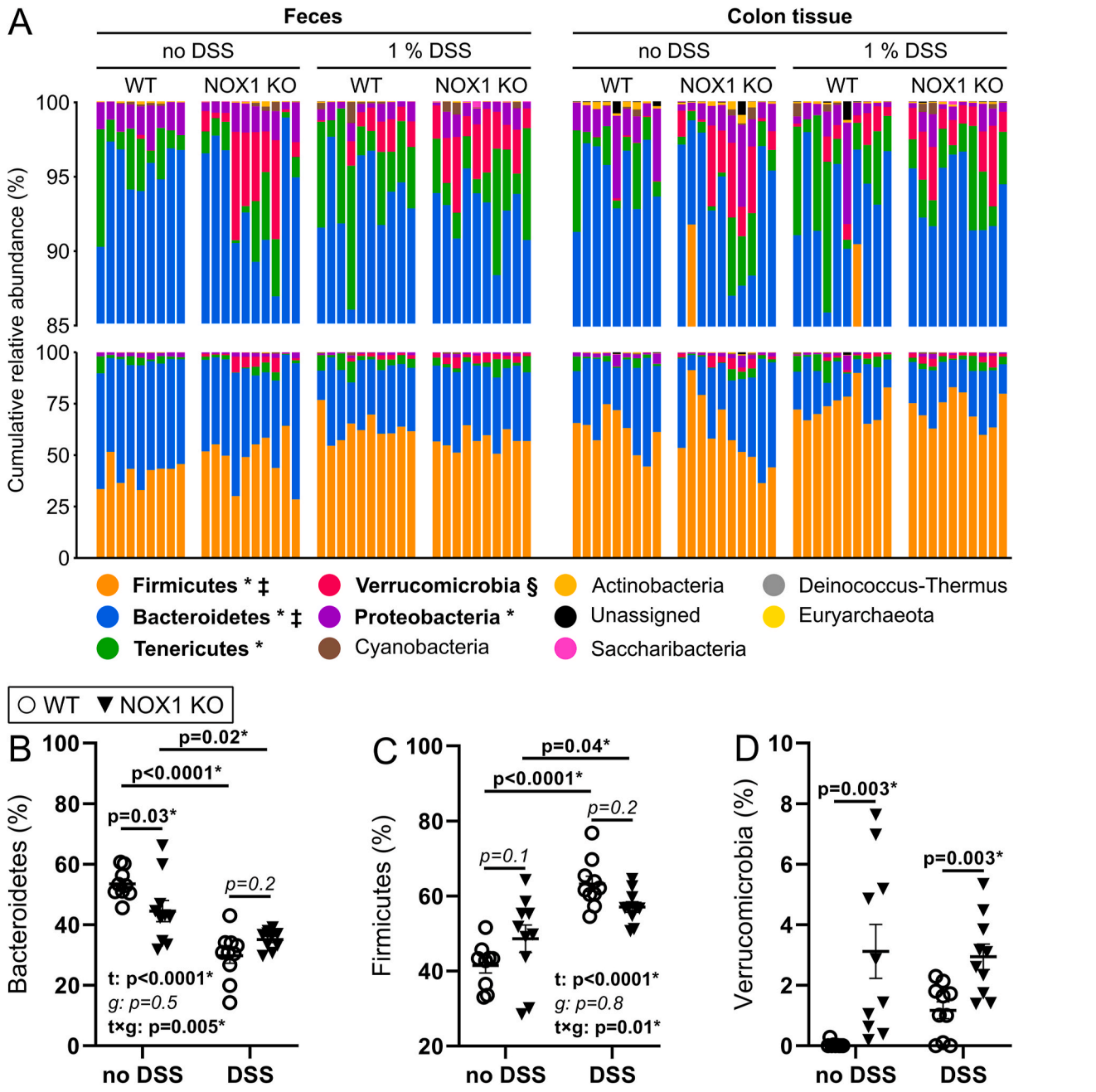

Fig. 7. Bacterial phyla characteristics of WT and NOX1 KO mice with or without 1% DSS treatment (6 days). (A) Cumulative relative abundance (%) of all detected phyla in individual feces and colon tissue samples. Phyla are sorted according to average abundance across all groups. Phyla in bold had average abundance above 1% in at least one group. *Indicates significant effect of DSS treatment for both feces and colon tissue, ‡ indicates significant interaction between genotype and treatment in feces, and § indicates higher abundance in NOX1 KO mice compared to WT mice in both feces and colon tissue. (B–D) Fecal relative abundance (%) of (B) Bacteroidetes, (C) Firmicutes, and (D) Verrucomicrobia. (B,C) P-values from 2-way ANOVA (main effect of treatment (t; no DSS versus 1% DSS) and genotype (g; WT versus NOX1 KO), and interaction effect (t×g)). Since significant interaction, p-values for simple main effects from post-hoc tests with Bonferroni correction for multiple comparisons are presented. *$p<0.05$. (D) Since 2-way ANOVA could not be performed due to heteroskedasticity and/or violation of normality assumption alternative tests were used within the two treatment groups: Fisher's exact test (no DSS) and *t*-test (DSS). Horizontal lines and whiskers are group mean ± SEM. n=9–10 per group. WT, wild type; NOX1, NADPH oxidase 1; KO, knockout; DSS, dextran sulfate sodium.

The abundance of the phylum Verrucomicrobia, completely dominated by genus *Akkermansia*, was much higher in NOX1 KO than in WT mice. However, 1% DSS treatment reduced the difference between the genotypes due to a bloom of *Akkermansia* in WT mice, in line with previous observations [69–73]. *Akkermansia* spp. are anaerobic mucus-associated commensal bacteria that feeds on mucus, reported to have beneficial roles in intestinal homeostasis [74,75] and wound repair [23]. However, their role in aggravation of intestinal inflammation is debated with somewhat conflicting results [76]. While some studies have shown that *Akkermansia* supplementation reduces inflammation induced by a high-fat diet [77,78], others have suggested that *Akkermansia* contributes to enhancing colitis [64,71]. Since DSS is known to cause structural changes of the inner mucus layer of the colon making it more available for bacterial penetration [79], this could explain the increase of *Akkermansia* after DSS treatment in WT mice. Coant *et al.* observed that NOX1 KO mice had an increased number of goblet cells, and consequently more mucus protein [24], which could explain the increase in *Akkermansia* abundance in NOX1 KO mice. However, the

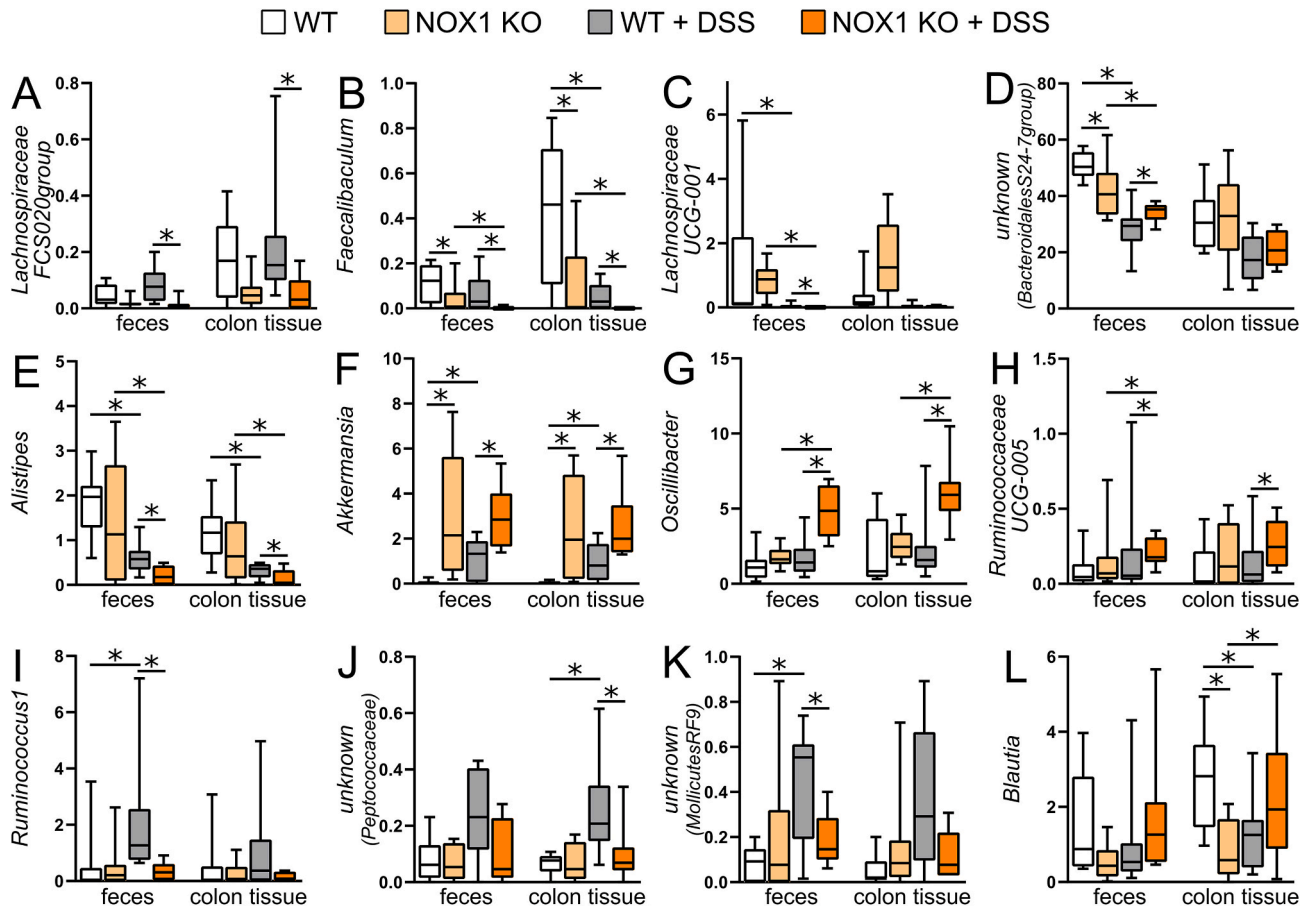

Fig. 8. Relative abundance (%) of abundant bacterial genera in feces and colon tissue from WT and NOX1 KO mice with or without 1% DSS treatment for (6 days). (A) *Lachnospiraceae FCS020 group*, (B) *Faecalibaculum*, (C) *Lachnospiraceae UCG-001*, (D) *unknown Bacteroidales S24-7group* (identical to family *Bacteroidales S24-7group*), (E) *Alistipes* (identical to family *Rikenellaceae*), (F) *Akkermansia* (identical to phylum Verrucomicrobia), (G) *Oscillibacter*, (H) *Ruminococcaceae UCG-005*, (I) *Ruminococcus1*, (J) *unknown Peptococcaceae*, (K) *unknown MollicutesRF9*, and (L) *Blautia*. n=9-10 per group. The presented genera are the ones that were found to have different abundance between WT and NOX1 KO mice in feces and/or colon tissue through LEfSe analysis (comparison of genotypes (WT, NOX1 KO) within each treatment (no DSS, 1% DSS), and between treatments within each genotype), and that had average relative abundance above 0.1% in feces and/or colon tissue. WT, wild type; NOX1, NADPH oxidase 1; KO, knockout; DSS, dextran sulfate sodium; LDA, linear discriminant analysis; LEfSe, LDA effect size. *Indicates the LEfSe-identified significant comparisons.

mucus seems to be unaffected by NOX1-deficiency in more recent studies [28,80]. Why *Akkermansia* in NOX1 KO mice seems unaffected by DSS remains unclear but is perhaps related to the less extensive increase in colonic ROS/RNS during inflammation in the NOX1-deficient mice.

The genus *Oscillibacter* (order Clostridiales in phylum Firmicutes) was highly increased in DSS-treated NOX1 KO mice, but not in WT mice. The fact that *Oscillibacter* abundance increases after antibiotic treatment [81] supports the notion that *Oscillibacter* spp. are opportunistic bacteria that thrive when the normal balance is disturbed. The implication of *Oscillibacter* abundance in health and disease seems unresolved, but studies of colon inflammation suggest that increased *Oscillibacter* abundance could be related to impaired barrier function [82], increased markers of colon inflammation [67,83], and increased colitis susceptibility [64]. Thus, high abundance of *Oscillibacter* in NOX1 KO mice after DSS treatment could be interpreted as a sign of increased disease.

The findings that both *Akkermansia* and *Oscillibacter* have higher abundances in the NOX1 KO mice may be attributed to changes in the redox environment caused by the NOX1-deficiency. Intriguingly, both *Akkermansia* and *Oscillibacter* increase in abundance following a polyphenol-rich diet [84]. As polyphenols are poorly taken up in the small intestine and therefore transported to the colon, it is plausible that they act as antioxidants there and thereby create a more reducing environment. To our knowledge, redox changes in NOX1 KO compared to WT mice have not been measured, but it is pertinent to speculate that such changes occur and lack of NOX1 will therefore favor the growth of *Akkermansia* and *Oscillibacter* in a reducing environment. The fact that *Oscillibacter* is only blooming in DSS-treated NOX1 KO mice and not in those not treated with DSS is not straightforward to explain. However, as mentioned above, *Oscillibacter* is probably opportunistic and will thrive when homeostasis is disturbed [81]. Thus, when a low dose of DSS is introduced, this stimulus is not sufficient to create a niche for *Oscillibacter* unless deficiency in NOX1 creates this unbalance.

As already discussed, in the experimental setup where we compare NOX1 KO and WT mice, it is not possible to assess the direct effects of NOX1-dependent ROS/RNS-deficiency on low-grade colon inflammation due to initial differences in the colonic microbiota between the genotypes prior to DSS treatment. Treating WT mice with ROS/RNS inhibitors could therefore be an alternative approach to investigate the impact of NOX1-dependent ROS/RNS formation during inflammation, avoiding the impact of genetic background. As peroxynitrite most likely is one of the major ROS/RNS-contributors during colon inflammation, formed by NOX-dependent superoxide and iNOS-dependent nitric oxide, the NOS inhibitor L-NAME could be a suitable candidate [8].

In conclusion, this study demonstrates that the superoxide-producing enzyme NOX1 is important for the formation of colonic extracellular ROS/RNS and modulates the colonic microbiota both during steady-state and in 1% DSS-induced colonic low-grade inflammation. Further,

while NOX1 offered no protection against pathological changes induced by low-grade inflammation, analyses of inflammation-associated genes indicated a trend for enhanced inflammation in NOX1-deficient mice which was further supported by the increment of LCN2. We therefore propose that NOX1-dependent ROS/RNS have a role in shaping the colonic microbiota, with potential beneficial consequences for intestinal health.

Author contributions

AMH, SDCR and HC: designed the study; AMH, SDCR, DP and HC: performed the experiments; AMH: conducted the statistical analyses; AMH, SDCR, DP, SKB and HC: interpreted the results; AMH, SDCR, SKB and HC: wrote the manuscript; AMH: prepared the figures for the manuscript; AMH, SDCR and HC: supervised the study; AMH, SDCR and HC: prepared the animal protocol; AMH, SDCR, SKB, DP, and HC: discussed the results and edited manuscript drafts; and all authors: read and approved the final manuscript.

Funding

This work was supported by PhD grants from the Faculty of Chemistry, Biotechnology and Food Science, NMBU.

Declaration of competing interest

None.

Acknowledgements

We thank Knut Rudi, Morten Nilsen, Inga Leena Angell, and Ida Ormaasen for providing lab facilities, technical support, and advice for 16S rRNA sequencing, Henriette Arnesen for methodological discussions on 16S sequencing data analyses, and Anders Kielland and Lars Fredrik Moen for practical help and discussion regarding mice experiments.

Appendix ASupplementary data

Supplementary data to this article can be found online at https://doi.org/10.1016/j.freeradbiomed.2022.06.234.

References

[1] T. Finkel, Oxygen radicals and signaling, Curr. Opin. Cell Biol. 10 (2) (1998) 248–253, https://doi.org/10.1016/s0955-0674(98)80147-6.
[2] M.J. Jackson, S. Papa, J. Bolanos, R. Bruckdorfer, H. Carlsen, R.M. Elliott, J. Flier, H.R. Griffiths, S. Heales, B. Holst, M. Lorusso, E. Lund, J. Oivind Moskaug, U. Moser, M. Di Paola, M.C. Polidori, A. Signorile, W. Stahl, J. Vina-Ribes, S. B. Astley, Antioxidants, reactive oxygen and nitrogen species, gene induction and mitochondrial function, Mol. Aspect. Med. 23 (1–3) (2002) 209–285, https://doi.org/10.1016/s0098-2997(02)00018-3.
[3] S.G. Rhee, Redox signaling: hydrogen peroxide as intracellular messenger, Exp. Mol. Med. 31 (2) (1999) 53–59, https://doi.org/10.1038/emm.1999.9.
[4] K. Bedard, K.H. Krause, The NOX family of ROS-generating NADPH oxidases: physiology and pathophysiology, Physiol. Rev. 87 (1) (2007) 245–313, https://doi.org/10.1152/physrev.00044.2005.
[5] C.C. Faria, R.S. Fortunato, The role of dual oxidases in physiology and cancer, Genet. Mol. Biol. 43 (1 suppl. 1) (2020), e20190096, https://doi.org/10.1590/1678-4685/GMB-2019-0096.
[6] T.L. Leto, M. Geiszt, Role of Nox family NADPH oxidases in host defense, Antioxidants Redox Signal. 8 (9–10) (2006) 1549–1561, https://doi.org/10.1089/ars.2006.8.1549.
[7] B. Rada, T.L. Leto, Oxidative innate immune defenses by Nox/Duox family NADPH oxidases, Contrib. Microbiol. 15 (2008) 164–187, https://doi.org/10.1159/000136357.
[8] C. Matziouridou, S.D.C. Rocha, O.A. Haabeth, K. Rudi, H. Carlsen, A. Kielland, iNOS- and NOX1-dependent ROS production maintains bacterial homeostasis in the ileum of mice, Mucosal Immunol. 11 (3) (2018) 774–784, https://doi.org/10.1038/mi.2017.106.
[9] T. Schwerd, R.V. Bryant, S. Pandey, M. Capitani, L. Meran, J.B. Cazier, J. Jung, K. Mondal, M. Parkes, C.G. Mathew, K. Fiedler, D.J. McCarthy, WGS500 Consortium, Oxford IBD cohort study investigators, COLORS in IBD group investigators, UK IBD Genetics Consortium, P.B. Sullivan, A. Rodrigues, S.P. L. Travis, C. Moore, J. Sambrook, W.H. Ouwehand, D.J. Roberts, J. Danesh, INTERVAL Study, R.K. Russell, D.C. Wilson, J.R. Kelsen, R. Cornall, L.A. Denson, S. Kugathasan, U.G. Knaus, E.G. Serra, C.A. Anderson, R.H. Duerr, D.P. McGovern, J. Cho, F. Powrie, V.S. Li, A.M. Muise, H.H. Uhlig, NOX1 loss-of-function genetic variants in patients with inflammatory bowel disease, Mucosal Immunol. 11 (2) (2018) 562–574, https://doi.org/10.1038/mi.2017.74.
[10] I. Szanto, L. Rubbia-Brandt, P. Kiss, K. Steger, B. Banfi, E. Kovari, F. Herrmann, A. Hadengue, K.H. Krause, Expression of NOX1, a superoxide-generating NADPH oxidase, in colon cancer and inflammatory bowel disease, J. Pathol. 207 (2) (2005) 164–176, https://doi.org/10.1002/path.1824.
[11] F. Moll, M. Walter, F. Rezende, V. Helfinger, E. Vasconez, T. De Oliveira, F. R. Greten, C. Olesch, A. Weigert, H.H. Radeke, K. Schroder, NoxO1 controls proliferation of colon epithelial cells, Front. Immunol. 9 (2018) 973, https://doi.org/10.3389/fimmu.2018.00973.
[12] M. Geiszt, K. Lekstrom, S. Brenner, S.M. Hewitt, R. Dana, H.L. Malech, T.L. Leto, NAD(P)H oxidase 1, a product of differentiated colon epithelial cells, can partially replace glycoprotein 91 phox in the regulated production of superoxide by phagocytes, J. Immunol. 171 (1) (2003) 299–306, https://doi.org/10.4049/jimmunol.171.1.299.
[13] H. Grasberger, J. Gao, H. Nagao-Kitamoto, S. Kitamoto, M. Zhang, N. Kamada, K. A. Eaton, M. El-Zaatari, A.B. Shreiner, J.L. Merchant, C. Owyang, J.Y. Kao, Increased expression of DUOX2 is an epithelial response to mucosal dysbiosis required for immune homeostasis in mouse intestine, Gastroenterology 149 (7) (2015) 1849–1859, https://doi.org/10.1053/j.gastro.2015.07.062.
[14] M. Kamizato, K. Nishida, K. Masuda, K. Takeo, Y. Yamamoto, T. Kawai, S. Teshima-Kondo, T. Tanahashi, K. Rokutan, Interleukin 10 inhibits interferon gamma- and tumor necrosis factor alpha-stimulated activation of NADPH oxidase 1 in human colonic epithelial cells and the mouse colon, J. Gastroenterol. 44 (12) (2009) 1172–1184, https://doi.org/10.1007/s00535-009-0119-6.
[15] G. Aviello, U.G. Knaus, NADPH oxidases and ROS signaling in the gastrointestinal tract, Mucosal Immunol. 11 (4) (2018) 1011–1023, https://doi.org/10.1038/s41385-018-0021-8.
[16] M. Kato, M. Marumo, J. Nakayama, M. Matsumoto, C. Yabe-Nishimura, T. Kamata, The ROS-generating oxidase Nox1 is required for epithelial restitution following colitis, Exp. Anim. 65 (3) (2016) 197–205, https://doi.org/10.1538/expanim.15-0127.
[17] R. Radi, Peroxynitrite, a stealthy biological oxidant, J. Biol. Chem. 288 (37) (2013) 26464–26472, https://doi.org/10.1074/jbc.R113.472936.
[18] H. Shaked, L.J. Hofseth, A. Chumanevich, A.A. Chumanevich, J. Wang, Y. Wang, K. Taniguchi, M. Guma, S. Shenouda, H. Clevers, C.C. Harris, M. Karin, Chronic epithelial NF-kappaB activation accelerates APC loss and intestinal tumor initiation through iNOS up-regulation, Proc. Natl. Acad. Sci. U. S. A. 109 (35) (2012) 14007–14012, https://doi.org/10.1073/pnas.1211509109.
[19] E. Larsson, V. Tremaroli, Y.S. Lee, O. Koren, I. Nookaew, A. Fricker, J. Nielsen, R. E. Ley, F. Backhed, Analysis of gut microbial regulation of host gene expression along the length of the gut and regulation of gut microbial ecology through MyD88, Gut 61 (8) (2012) 1124–1131, https://doi.org/10.1136/gutjnl-2011-301104.
[20] J.O. Lundberg, E. Weitzberg, Biology of nitrogen oxides in the gastrointestinal tract, Gut 62 (4) (2013) 616–629, https://doi.org/10.1136/gutjnl-2011-301649.
[21] X. Treton, E. Pedruzzi, C. Guichard, Y. Ladeiro, S. Sedghi, M. Vallee, N. Fernandez, E. Bruyere, P.L. Woerther, R. Ducroc, N. Montcuquet, J.N. Freund, I. Van Seuningen, F. Barreau, A. Marah, J.P. Hugot, D. Cazals-Hatem, Y. Bouhnik, F. Daniel, E. Ogier-Denis, Combined NADPH oxidase 1 and interleukin 10 deficiency induces chronic endoplasmic reticulum stress and causes ulcerative colitis-like disease in mice, PLoS One 9 (7) (2014), e101669, https://doi.org/10.1371/journal.pone.0101669.
[22] G. Leoni, A. Alam, P.A. Neumann, J.D. Lambeth, G. Cheng, J. McCoy, R.S. Hilgarth, K. Kundu, N. Murthy, D. Kusters, C. Reutelingsperger, M. Perretti, C.A. Parkos, A. S. Neish, A. Nusrat, Annexin A1, formyl peptide receptor, and NOX1 orchestrate epithelial repair, J. Clin. Invest. 123 (1) (2013) 443–454, https://doi.org/10.1172/JCI65831.
[23] A. Alam, G. Leoni, M. Quiros, H. Wu, C. Desai, H. Nishio, R.M. Jones, A. Nusrat, A. S. Neish, The microenvironment of injured murine gut elicits a local pro-restitutive microbiota, Nat Microbiol 1 (2016) 15021, https://doi.org/10.1038/nmicrobiol.2015.21.
[24] N. Coant, S. Ben Mkaddem, E. Pedruzzi, C. Guichard, X. Treton, R. Ducroc, J. N. Freund, D. Cazals-Hatem, Y. Bouhnik, P.L. Woerther, D. Skurnik, A. Grodet, M. Fay, D. Biard, T. Lesuffleur, C. Deffert, R. Moreau, A. Groyer, K.H. Krause, F. Daniel, E. Ogier-Denis, NADPH oxidase 1 modulates WNT and NOTCH1 signaling to control the fate of proliferative progenitor cells in the colon, Mol. Cell Biol. 30 (11) (2010) 2636–2650, https://doi.org/10.1128/MCB.01194-09.
[25] R.M. Jones, L. Luo, C.S. Ardita, A.N. Richardson, Y.M. Kwon, J.W. Mercante, A. Alam, C.L. Gates, H. Wu, P.A. Swanson, J.D. Lambeth, P.W. Denning, A.S. Neish, Symbiotic lactobacilli stimulate gut epithelial proliferation via Nox-mediated generation of reactive oxygen species, EMBO J. 32 (23) (2013) 3017–3028, https://doi.org/10.1038/emboj.2013.224.
[26] R.M. Jones, A.S. Neish, Redox signaling mediated by the gut microbiota, Free Radic.Biol & med. (2016), https://doi.org/10.1016/j.freeradbiomed.2016.10.495.
[27] A. Kielland, T. Blom, K.S. Nandakumar, R. Holmdahl, R. Blomhoff, H. Carlsen, In vivo imaging of reactive oxygen and nitrogen species in inflammation using the luminescent probe L-012, Free Radic.Biol & med. 47 (6) (2009) 760–766, https://doi.org/10.1016/j.freeradbiomed.2009.06.013.
[28] G. Aviello, A.K. Singh, S. O'Neill, E. Conroy, W. Gallagher, G. D'Agostino, A. W. Walker, B. Bourke, D. Scholz, U.G. Knaus, Colitis susceptibility in mice with reactive oxygen species deficiency is mediated by mucus barrier and immune

defense defects, Mucosal Immunol. 12 (6) (2019) 1316–1326, https://doi.org/10.1038/s41385-019-0205-x.
[29] B. Chassaing, A.T. Gewirtz, Gut microbiota, low-grade inflammation, and metabolic syndrome, Toxicol. Pathol. 42 (1) (2014) 49–53, https://doi.org/10.1177/0192623313508481.
[30] A. Agus, J. Denizot, J. Thevenot, M. Martinez-Medina, S. Massier, P. Sauvanet, A. Bernalier-Donadille, S. Denis, P. Hofman, R. Bonnet, E. Billard, N. Barnich, Western diet induces a shift in microbiota composition enhancing susceptibility to Adherent-Invasive *E. coli* infection and intestinal inflammation, Sci. Rep. 6 (2016), 19032, https://doi.org/10.1038/srep19032.
[31] G. Barbara, C. Cremon, V. Stanghellini, Inflammatory bowel disease and irritable bowel syndrome: similarities and differences, Curr. Opin. Gastroenterol. 30 (4) (2014) 352–358, https://doi.org/10.1097/MOG.0000000000000070.
[32] B. Chassaing, O. Koren, J.K. Goodrich, A.C. Poole, S. Srinivasan, R.E. Ley, A. T. Gewirtz, Dietary emulsifiers impact the mouse gut microbiota promoting colitis and metabolic syndrome, Nature 519 (7541) (2015) 92–96, https://doi.org/10.1038/nature14232.
[33] A.C. Moss, The meaning of low-grade inflammation in clinically quiescent inflammatory bowel disease, Curr. Opin. Gastroenterol. 30 (4) (2014) 365–369, https://doi.org/10.1097/MOG.0000000000000082.
[34] B. Chassaing, G. Srinivasan, M.A. Delgado, A.N. Young, A.T. Gewirtz, M. Vijay-Kumar, Fecal lipocalin 2, a sensitive and broadly dynamic non-invasive biomarker for intestinal inflammation, PLoS One 7 (9) (2012), e44328, https://doi.org/10.1371/journal.pone.0044328.
[35] R. Suzuki, H. Kohno, S. Sugie, H. Nakagama, T. Tanaka, Strain differences in the susceptibility to azoxymethane and dextran sodium sulfate-induced colon carcinogenesis in mice, Carcinogenesis 27 (1) (2006) 162–169, https://doi.org/10.1093/carcin/bgi205.
[36] B. Chassaing, J.D. Aitken, M. Malleshappa, M. Vijay-Kumar, Dextran sulfate sodium (DSS)-induced colitis in mice, Curr. Protoc. Im. 104 (2014) 15.25.1–15.25.14, https://doi.org/10.1002/0471142735.im1525s104.
[37] F.I. Umoh, I. Kato, J. Ren, P.L. Wachowiak, M.T.t. Ruffin, D.K. Turgeon, A. Sen, D. E. Brenner, Z. Djuric, Markers of systemic exposures to products of intestinal bacteria in a dietary intervention study, Eur. J. Nutr. 55 (2) (2016) 793–798, https://doi.org/10.1007/s00394-015-0900-7.
[38] A.B. Bialkowska, A.M. Ghaleb, M.O. Nandan, V.W. Yang, Improved Swiss-rolling technique for intestinal tissue preparation for immunohistochemical and immunofluorescent analyses, J Vis Exp 113 (2016), e54161, https://doi.org/10.3791/54161.
[39] T.A. Kerr, M.A. Ciorba, H. Matsumoto, V.R. Davis, J. Luo, S. Kennedy, Y. Xie, A. Shaker, B.K. Dieckgraefe, N.O. Davidson, Dextran sodium sulfate inhibition of real-time polymerase chain reaction amplification: a poly-A purification solution, Inflamm. Bowel Dis. 18 (2) (2012) 344–348, https://doi.org/10.1002/ibd.21763.
[40] E. Viennois, F. Chen, H. Laroui, M.T. Baker, D. Merlin, Dextran sodium sulfate inhibits the activities of both polymerase and reverse transcriptase: lithium chloride purification, a rapid and efficient technique to purify RNA, BMC Res. Notes 6 (2013) 360, https://doi.org/10.1186/1756-0500-6-360.
[41] J.M. Ruijter, C. Ramakers, W.M. Hoogaars, Y. Karlen, O. Bakker, M.J. van den Hoff, A.F. Moorman, Amplification efficiency: linking baseline and bias in the analysis of quantitative PCR data, Nucleic Acids Res. 37 (6) (2009) e45, https://doi.org/10.1093/nar/gkp045.
[42] E. Avershina, K. Lundgard, M. Sekelja, C. Dotterud, O. Storro, T. Oien, R. Johnsen, K. Rudi, Transition from infant- to adult-like gut microbiota, Environ. Microbiol. 18 (7) (2016) 2226–2236, https://doi.org/10.1111/1462-2920.13248.
[43] J.G. Caporaso, J. Kuczynski, J. Stombaugh, K. Bittinger, F.D. Bushman, E. K. Costello, N. Fierer, A.G. Pena, J.K. Goodrich, J.I. Gordon, G.A. Huttley, S. T. Kelley, D. Knights, J.E. Koenig, R.E. Ley, C.A. Lozupone, D. McDonald, B. D. Muegge, M. Pirrung, J. Reeder, J.R. Sevinsky, P.J. Turnbaugh, W.A. Walters, J. Widmann, T. Yatsunenko, J. Zaneveld, R. Knight, QIIME allows analysis of high-throughput community sequencing data, Nat. Methods 7 (5) (2010) 335–336, https://doi.org/10.1038/nmeth.f.303.
[44] R.C. Edgar, Search and clustering orders of magnitude faster than BLAST, Bioinformatics 26 (19) (2010) 2460–2461, https://doi.org/10.1093/bioinformatics/btq461.
[45] R.C. Edgar, UPARSE: highly accurate OTU sequences from microbial amplicon reads, Nat. Methods 10 (10) (2013) 996–998, https://doi.org/10.1038/nmeth.2604.
[46] E. Pruesse, C. Quast, K. Knittel, B.M. Fuchs, W. Ludwig, J. Peplies, F.O. Glockner, SILVA: a comprehensive online resource for quality checked and aligned ribosomal RNA sequence data compatible with ARB, Nucleic Acids Res. 35 (21) (2007) 7188–7196, https://doi.org/10.1093/nar/gkm864.
[47] C.A. Lozupone, M. Hamady, S.T. Kelley, R. Knight, Quantitative and qualitative beta diversity measures lead to different insights into factors that structure microbial communities, Appl. Environ. Microbiol. 73 (5) (2007) 1576–1585, https://doi.org/10.1128/AEM.01996-06.
[48] R Core Team, R, A Language and Environment for Statistical Computing (Version 4.1.2), R Foundation for Statistical Computing, Vienna, Austria, 2021. https://www.R-project.org/.
[49] J. Oksanen, F.G. Blanchet, M. Friendly, R. Kindt, P. Legendre, D. McGlinn, P. R. Minchin, R.B. O'Hara, G.L. Simpson, P. Solymos, M.H.H. Stevens, E. Szoecs, H. Wagner, Vegan: Community Ecology Package (Version 2.5-7), 2020. https://CRAN.R-project.org/package=vegan.
[50] M. Hervé, RVAideMemoire: Testing and Plotting Procedures for Biostatistics (Version 0.9-79), 2021. https://CRAN.R-project.org/package=RVAideMemoire.
[51] N. Segata, J. Izard, L. Waldron, D. Gevers, L. Miropolsky, W.S. Garrett, C. Huttenhower, Metagenomic biomarker discovery and explanation, Genome Biol. 12 (6) (2011) R60, https://doi.org/10.1186/gb-2011-12-6-r60.
[52] S. Gross, S.T. Gammon, B.L. Moss, D. Rauch, J. Harding, J.W. Heinecke, L. Ratner, D. Piwnica-Worms, Bioluminescence imaging of myeloperoxidase activity in vivo, Nat. Med. 15 (4) (2009) 455–461, https://doi.org/10.1038/nm.1886.
[53] A. Daiber, M. Oelze, S. Steven, S. Kroller-Schon, T. Munzel, Taking up the cudgels for the traditional reactive oxygen and nitrogen species detection assays and their use in the cardiovascular system, Redox Biol. 12 (2017) 35–49, https://doi.org/10.1016/j.redox.2017.02.001.
[54] K. Van Dyke, E. Ghareeb, M. Van Dyke, D.H. Van Thiel, Ultrasensitive peroxynitrite-based luminescence with L-012 as a screening system for antioxidative/antinitrating substances, e.g. Tylenol (acetaminophen), 4-OH tempol, quercetin and carboxy-PTIO, Luminescence 22 (4) (2007) 267–274, https://doi.org/10.1002/bio.959.
[55] R.J. Goiffon, S.C. Martinez, D. Piwnica-Worms, A rapid bioluminescence assay for measuring myeloperoxidase activity in human plasma, Nat. Commun. 6 (2015) 6271, https://doi.org/10.1038/ncomms7271.
[56] J. Zielonka, J.D. Lambeth, B. Kalyanaraman, On the use of L-012, a luminol-based chemiluminescent probe, for detecting superoxide and identifying inhibitors of NADPH oxidase: a reevaluation, Free Radic.Biol & med. 65 (2013) 1310–1314, https://doi.org/10.1016/j.freeradbiomed.2013.09.017.
[57] A. Daiber, M. August, S. Baldus, M. Wendt, M. Oelze, K. Sydow, A.L. Kleschyov, T. Munzel, Measurement of NAD(P)H oxidase-derived superoxide with the luminol analogue L-012, Free Radic.Biol & med. 36 (1) (2004) 101–111, https://doi.org/10.1016/j.freeradbiomed.2003.10.012.
[58] H. Yokota, A. Tsuzuki, Y. Shimada, A. Imai, D. Utsumi, T. Tsukahara, M. Matsumoto, K. Amagase, K. Iwata, A. Nakamura, C. Yabe-Nishimura, S. Kato, NOX1/NADPH oxidase expressed in colonic macrophages contributes to the pathogenesis of colonic inflammation in trinitrobenzene sulfonic acid-induced murine colitis, J Pharmacol Exp Ther 360 (1) (2017) 192–200, https://doi.org/10.1124/jpet.116.235580.
[59] D. Liu, J.C. Marie, A.L. Pelletier, Z. Song, M. Ben-Khemis, K. Boudiaf, C. Pintard, T. Leger, S. Terrier, G. Chevreux, J. El-Benna, P.M. Dang, Protein kinase CK2 acts as a molecular brake to control NADPH oxidase 1 activation and colon inflammation, Cell Mol Gastroenterol Hepatol 13 (4) (2022) 1073–1093, https://doi.org/10.1016/j.jcmgh.2022.01.003.
[60] V. Singh, B.S. Yeoh, B. Chassaing, B. Zhang, P. Saha, X. Xiao, D. Awasthi, R. Shashidharamurthy, M. Dikshit, A. Gewirtz, M. Vijay-Kumar, Microbiota-inducible innate immune, siderophore binding protein lipocalin 2 is critical for intestinal homeostasis, Cell Mol Gastroenterol Hepatol 2 (4) (2016) 482–498, https://doi.org/10.1016/j.jcmgh.2016.03.007, e6.
[61] R.M. Jones, C. Desai, T.M. Darby, L. Luo, A.A. Wolfarth, C.D. Scharer, C.S. Ardita, A.R. Reedy, E.S. Keebaugh, A.S. Neish, Lactobacilli modulate epithelial cytoprotection through the Nrf2 pathway, Cell Rep. 12 (8) (2015) 1217–1225, https://doi.org/10.1016/j.celrep.2015.07.042.
[62] T.O. Khor, M.T. Huang, K.H. Kwon, J.Y. Chan, B.S. Reddy, A.N. Kong, Nrf2-deficient mice have an increased susceptibility to dextran sulfate sodium-induced colitis, Cancer Res. 66 (24) (2006) 11580–11584, https://doi.org/10.1158/0008-5472.CAN-06-3562.
[63] W. Gao, L. Guo, Y. Yang, Y. Wang, S. Xia, H. Gong, B.K. Zhang, M. Yan, Dissecting the crosstalk between Nrf2 and NF-κB response pathways in drug-induced toxicity, Front. Cell Dev. Biol. 9 (2021), 809952, https://doi.org/10.3389/fcell.2021.809952.
[64] M. Li, Y. Wu, Y. Hu, L. Zhao, C. Zhang, Initial gut microbiota structure affects sensitivity to DSS-induced colitis in a mouse model, Sci. China Life Sci. 61 (7) (2018) 762–769, https://doi.org/10.1007/s11427-017-9097-0.
[65] C.B. Van Buiten, G. Wu, Y.Y. Lam, L. Zhao, I. Raskin, Elemental iron modifies the redox environment of the gastrointestinal tract: a novel therapeutic target and test for metabolic syndrome, Free Radic.Biol & med. 168 (2021) 203–213, https://doi.org/10.1016/j.freeradbiomed.2021.03.032.
[66] A. Karkman, J. Lehtimaki, L. Ruokolainen, The ecology of human microbiota: dynamics and diversity in health and disease, Ann. N. Y. Acad. Sci. 1399 (1) (2017) 78–92, https://doi.org/10.1111/nyas.13326.
[67] M. Wu, P. Li, Y. An, J. Ren, D. Yan, J. Cui, D. Li, M. Li, M. Wang, G. Zhong, Phloretin ameliorates dextran sulfate sodium-induced ulcerative colitis in mice by regulating the gut microbiota, Pharmacol. Res. 150 (2019), 104489, https://doi.org/10.1016/j.phrs.2019.104489.
[68] R. Dziarski, S.Y. Park, D.R. Kashyap, S.E. Dowd, D. Gupta, Pglyrp-regulated gut microflora prevotella falsenii, parabacteroides distasonis and Bacteroides eggerthii enhance and Alistipes finegoldii attenuates colitis in mice, PLoS One 11 (1) (2016), e0146162, https://doi.org/10.1371/journal.pone.0146162.
[69] C. Schwab, D. Berry, I. Rauch, I. Rennisch, J. Ramesmayer, E. Hainzl, S. Heider, T. Decker, L. Kenner, M. Muller, B. Strobl, M. Wagner, C. Schleper, A. Loy, T. Urich, Longitudinal study of murine microbiota activity and interactions with the host during acute inflammation and recovery, ISME J. 8 (5) (2014) 1101–1114, https://doi.org/10.1038/ismej.2013.223.
[70] D. Berry, C. Schwab, G. Milinovich, J. Reichert, K. Ben Mahfoudh, T. Decker, M. Engel, B. Hai, E. Hainzl, S. Heider, L. Kenner, M. Muller, I. Rauch, B. Strobl, M. Wagner, C. Schleper, T. Urich, A. Loy, Phylotype-level 16S rRNA analysis reveals new bacterial indicators of health state in acute murine colitis, ISME J. 6 (11) (2012) 2091–2106, https://doi.org/10.1038/ismej.2012.39.
[71] Q. Zhang, Y. Wu, J. Wang, G. Wu, W. Long, Z. Xue, L. Wang, X. Zhang, X. Pang, Y. Zhao, L. Zhao, C. Zhang, Accelerated dysbiosis of gut microbiota during aggravation of DSS-induced colitis by a butyrate-producing bacterium, Sci. Rep. 6 (2016) 27572, https://doi.org/10.1038/srep27572.

[72] G. Lo Sasso, B.W. Phillips, A. Sewer, J.N.D. Battey, A. Kondylis, M. Talikka, B. Titz, E. Guedj, D. Peric, D. Bornand, R. Dulize, C. Merg, M. Corciulo, S. Ouadi, R. Yanuar, C.K. Tung, N.V. Ivanov, M.C. Peitsch, J. Hoeng, The reduction of DSS-induced colitis severity in mice exposed to cigarette smoke is linked to immune modulation and microbial shifts, Sci. Rep. 10 (1) (2020) 3829, https://doi.org/10.1038/s41598-020-60175-3.

[73] M.A. Borton, A. Sabag-Daigle, J. Wu, L.M. Solden, B.S. O'Banion, R.A. Daly, R. A. Wolfe, J.F. Gonzalez, V.H. Wysocki, B.M.M. Ahmer, K.C. Wrighton, Chemical and pathogen-induced inflammation disrupt the murine intestinal microbiome, Microbiome 5 (1) (2017) 47, https://doi.org/10.1186/s40168-017-0264-8.

[74] M. Derrien, P. Van Baarlen, G. Hooiveld, E. Norin, M. Muller, W.M. de Vos, Modulation of mucosal immune response, tolerance, and proliferation in mice colonized by the mucin-degrader Akkermansia muciniphila, Front. Microbiol. 2 (2011) 166, https://doi.org/10.3389/fmicb.2011.00166.

[75] M. Derrien, M.C. Collado, K. Ben-Amor, S. Salminen, W.M. de Vos, The Mucin degrader Akkermansia muciniphila is an abundant resident of the human intestinal tract, Appl. Environ. Microbiol. 74 (5) (2008) 1646–1648, https://doi.org/10.1128/AEM.01226-07.

[76] T. Zhang, X. Ji, G. Lu, F. Zhang, The potential of Akkermansia muciniphila in inflammatory bowel disease, Appl. Microbiol. Biotechnol. 105 (14–15) (2021) 5785–5794, https://doi.org/10.1007/s00253-021-11453-1.

[77] A. Everard, C. Belzer, L. Geurts, J.P. Ouwerkerk, C. Druart, L.B. Bindels, Y. Guiot, M. Derrien, G.G. Muccioli, N.M. Delzenne, W.M. de Vos, P.D. Cani, Cross-talk between *Akkermansia muciniphila* and intestinal epithelium controls diet-induced obesity, Proc. Natl. Acad. Sci. U. S. A. 110 (22) (2013) 9066–9071, https://doi.org/10.1073/pnas.1219451110.

[78] N.R. Shin, J.C. Lee, H.Y. Lee, M.S. Kim, T.W. Whon, M.S. Lee, J.W. Bae, An increase in the Akkermansia spp. population induced by metformin treatment improves glucose homeostasis in diet-induced obese mice, Gut 63 (5) (2014) 727–735, https://doi.org/10.1136/gutjnl-2012-303839.

[79] M.E. Johansson, J.K. Gustafsson, K.E. Sjoberg, J. Petersson, L. Holm, H. Sjovall, G. C. Hansson, Bacteria penetrate the inner mucus layer before inflammation in the dextran sulfate colitis model, PLoS One 5 (8) (2010), e12238, https://doi.org/10.1371/journal.pone.0012238.

[80] G. Pircalabioru, G. Aviello, M. Kubica, A. Zhdanov, M.H. Paclet, L. Brennan, R. Hertzberger, D. Papkovsky, B. Bourke, U.G. Knaus, Defensive mutualism rescues NADPH oxidase inactivation in gut infection, Cell Host Microbe 19 (5) (2016) 651–663, https://doi.org/10.1016/j.chom.2016.04.007.

[81] H. Yan, B. Yu, J. Degroote, T. Spranghers, N. Van Noten, M. Majdeddin, M. Van Poucke, L. Peelman, J. De Vrieze, N. Boon, I. Gielen, S. Smet, D. Chen, J. Michiels, Antibiotic affects the gut microbiota composition and expression of genes related to lipid metabolism and myofiber types in skeletal muscle of piglets, BMC Vet. Res. 16 (1) (2020) 392, https://doi.org/10.1186/s12917-020-02592-0.

[82] Y.Y. Lam, C.W. Ha, C.R. Campbell, A.J. Mitchell, A. Dinudom, J. Oscarsson, D. I. Cook, N.H. Hunt, I.D. Caterson, A.J. Holmes, L.H. Storlien, Increased gut permeability and microbiota change associate with mesenteric fat inflammation and metabolic dysfunction in diet-induced obese mice, PLoS One 7 (3) (2012), e34233, https://doi.org/10.1371/journal.pone.0034233.

[83] Y. Peng, Y. Yan, P. Wan, D. Chen, Y. Ding, L. Ran, J. Mi, L. Lu, Z. Zhang, X. Li, X. Zeng, Y. Cao, Gut microbiota modulation and anti-inflammatory properties of anthocyanins from the fruits of Lycium ruthenicum Murray in dextran sodium sulfate-induced colitis in mice, Free Radic.Biol & med. 136 (2019) 96–108, https://doi.org/10.1016/j.freeradbiomed.2019.04.005.

[84] F.F. Anhe, T.V. Varin, M. Le Barz, G. Pilon, S. Dudonne, J. Trottier, P. St-Pierre, C. S. Harris, M. Lucas, M. Lemire, E. Dewailly, O. Barbier, Y. Desjardins, D. Roy, A. Marette, Arctic berry extracts target the gut-liver axis to alleviate metabolic endotoxaemia, insulin resistance and hepatic steatosis in diet-induced obese mice, Diabetologia 61 (4) (2018) 919–931, https://doi.org/10.1007/s00125-017-4520-z.

[85] G. Gavazzi, B. Banfi, C. Deffert, L. Fiette, M. Schappi, F. Herrmann, K.H. Krause, Decreased blood pressure in NOX1-deficient mice, FEBS Lett 580 (2) (2006) 497–504, https://doi.org/10.1016/j.febslet.2005.12.049.